Research Square

Preprints are preliminary reports that have not undergone peer review.
They should not be considered conclusive, used to inform clinical practice,
or referenced by the media as validated information.

Reliability T-Spherical Fuzzy Aczél–Alsina Sine-Trigonometric Aggregation Operators for Smart Waste Management Intervention Prioritization: A Case Study in Delhi, India

Subramanian Petchimuthu
University College of Engineering Nagercoil, Anna University
Meena Somasundaram
meenaprem14@gmail.com
KPR Institute of Engineering and Technology
Fathima Banu
Suresh Kumar
C.S.I Institute of Technology

Research Article

Keywords: Reliability T-Spherical Fuzzy Set, Aczél–Alsina Sine-Trigonometric Aggregation Operators; Multi-Attribute Group Decision Making, Smart Waste Management, Decision Support

Posted Date: November 23rd, 2026

DOI: https://doi.org/10.21203/rs.3.rs-11072449/v1

License: This work is licensed under a Creative Commons Attribution 4.0 International License.
Read Full License

Additional Declarations: No competing interests reported.

Reliability T-Spherical Fuzzy Aczél–Alsina Sine-Trigonometric Aggregation Operators for Smart Waste Management Intervention Prioritization: A Case Study in Delhi, India

Subramanian Petchimuthu[a], Meena Somasundaram[b,*], Fathima Banu M[a], Suresh Kumar R[c]

[a] *Department of Science and Humanities (Mathematics), University College of Engineering Nagercoil, Nagercoil-629004, Anna University, Tamil Nadu, India*
[b] *Department of Mathematics, KPR Institute of Engineering and Technology, Coimbatore-641407, Tamil Nadu, India*
[c] *Department of Science and Humanities (Mathematics), C.S.I. Institute of Technology, Thovalai-629302,Tamil Nadu, India*

Abstract

Prioritizing smart waste management interventions to reduce untreated municipal waste is a complex multi-attribute group decision-making (MAGDM) problem involving uncertain and reliability-sensitive expert assessments. Although existing fuzzy models effectively represent uncertainty, they generally fail to simultaneously capture membership information (MI), abstinence information (AbI), non-membership information (NMI), and the reliability of these assessments within a unified framework. To address this limitation, this paper proposes the Reliability T-Spherical Fuzzy Set (RT-SFS), a reliability-aware extension of the conventional T-spherical fuzzy framework that associates independent reliability degrees with MI, AbI, and NMI while preserving the underlying T-spherical fuzzy structure. Based on RT-SFS, a family of Aczél–Alsina Sine-Trigonometric aggregation operators is developed, including weighted averaging, weighted geometric, ordered weighted averaging, and ordered weighted geometric operators. These operators combine Aczél–Alsina aggregation mechanisms with sine-trigonometric operational laws to flexibly model diverse decision-makers' risk attitudes while enhancing information discrimination. A corresponding MAGDM methodology is established and applied to prioritize smart waste management interventions in Delhi, India. Sensitivity, ablation, and comparative analyses demonstrate the robustness, stability, and enhanced discrimination capability of the proposed approach. The proposed framework provides an effective decision-support tool for sustainable urban waste management planning and extends T-spherical fuzzy decision-making to reliability-aware MAGDM problems.

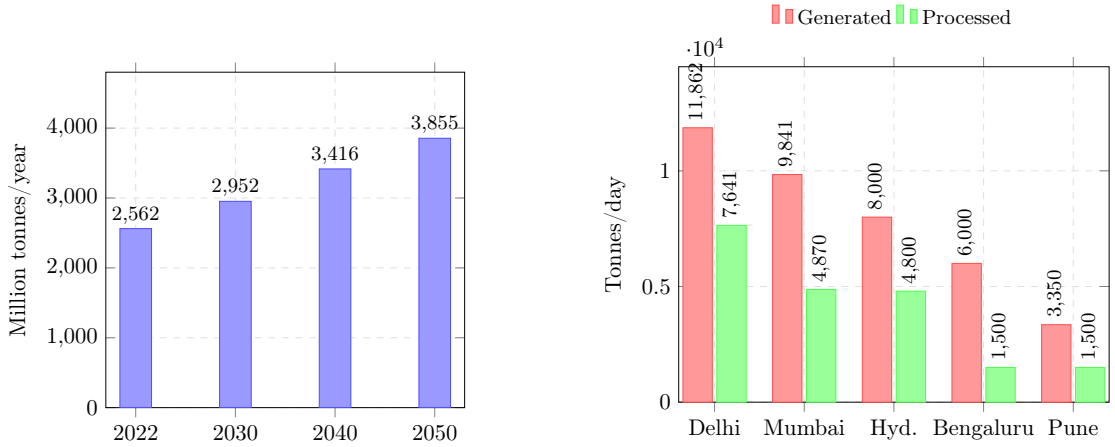
Keywords: Reliability T-Spherical Fuzzy Set; Aczél–Alsina Sine-Trigonometric Aggregation Operators; Multi-Attribute Group Decision Making; Smart Waste Management; Decision Support

1. Introduction

Municipal solid waste (MSW) management has become a major global challenge. According to the latest World Bank data [1], global MSW generation reached 2.56 billion tonnes in 2022 and is projected to increase to 3.86 billion tonnes by 2050, representing a 50% increase within less than three decades (Fig. 1a). Inefficient MSW management poses serious environmental, public health, and sustainability risks. Owing to rapid population growth from 0.35 billion in 1950 to 1.48 billion in 2026, developing countries such as India face increasing challenges in managing MSW [2]. Major Indian cities generate substantial quantities of municipal waste, yet their waste-processing capacities remain inadequate (Fig. 1b). Among these cities, Delhi currently generates approximately 11,862 tonnes of municipal waste daily, of which nearly 35.6% remains untreated despite ongoing investments in waste-processing infrastructure [3]. This substantial treatment gap highlights the urgent need to improve collection efficiency, waste processing, and resource recovery through appropriate smart waste management interventions. However, financial, technical, operational, and infrastructural constraints often prevent municipal authorities from implementing all available smart waste management interventions simultaneously. Consequently, prioritizing the most appropriate smart waste management interventions has become an important multi-attribute group

*Corresponding author.
Email addresses: svmuthu1983@gmail.com (Subramanian Petchimuthu), meenaprem14@gmail.com (Meena Somasundaram), fathimams1999@gmail.com (Fathima Banu M), sureshcsiit1973@gmail.com (Suresh Kumar R)

decision-making (MAGDM) problem involving multiple conflicting technical, economic, environmental, and social criteria.



(a) Global MSW Projection

(b) Indian Urban Processing Gap (2025–26)

Figure 1: Motivation for smart waste management intervention prioritization. (a) Projected global municipal solid waste (MSW) generation from 2022 to 2050 based on World Bank estimates [1]. (b) Comparison of daily municipal waste generation and processing capacities across selected major Indian cities during 2025–2026 [3, 4, 5, 6].

To address these challenges, several smart waste management (SWM) interventions have been proposed to improve collection efficiency, treatment performance, and resource recovery. Representative interventions include IoT-enabled smart bin deployment, IoT-based waste monitoring systems, AI-driven route optimization, automated waste-sorting facilities, and waste-to-energy technologies [7]. Selecting an appropriate intervention requires balancing multiple conflicting criteria, including implementation cost, operational efficiency, environmental sustainability, scalability, public acceptance, and maintenance complexity. Moreover, expert assessments are often characterized by uncertainty, abstention, and varying degrees of reliability, making reliability-aware information aggregation essential for robust decision-making. Thus, SWM intervention prioritization is a complex MAGDM problem that requires effective uncertainty modeling and reliability-aware information aggregation.

Given the inherent uncertainty in MAGDM, fuzzy set theory has evolved from classical membership information (MI) models [8] to frameworks incorporating non-membership information (NMI), including intuitionistic fuzzy sets (IFSs) [9], Pythagorean fuzzy sets (PyFSs) [10], and $\mathfrak{q}$-rung orthopair fuzzy sets ($\mathfrak{q}$-ROFSs) [11]. To provide richer representations of uncertainty, picture fuzzy sets (PFSs) [12], spherical fuzzy sets (SFSs), and T-spherical fuzzy sets (T-SFSs) [13] further incorporate abstinence information (AbI). Although T-SFSs effectively represent MI, AbI, and NMI, they implicitly assume equal reliability across assessments. In practical MAGDM, however, assessment reliability may vary owing to differences in domain expertise, information availability, data quality, and technological maturity. Consequently, conventional T-SFSs cannot distinguish between highly reliable and less reliable assessments. In contrast, linear Diophantine fuzzy sets (LDFSs) [14] and $\mathfrak{q}$-rung linear Diophantine fuzzy sets ($\mathfrak{q}$-RLDFSs) [15] introduced reference parameters to characterize assessment reliability. However, these frameworks do not directly provide a unified representation of MI, AbI, NMI, and their corresponding reliability degrees (RDs). To address related representational limitations, Scaled $\mathfrak{q}$-Rung Orthopair Fuzzy Sets (Sq-ROFSs) were proposed [16]. However, Sq-ROFSs do not incorporate AbI and therefore cannot simultaneously represent MI, AbI, NMI, and their corresponding RDs within a unified framework. Motivated by this gap, this study proposes the Reliability T-Spherical Fuzzy Set (RT-SFS), a reliability-aware extension of T-SFS that simultaneously represents MI, AbI, NMI, and their corresponding RDs. The proposed RT-SFS establishes a unified reliability-aware fuzzy environment through new operational laws, aggregation operators (AOs), ranking measures, and a MAGDM framework, while preserving T-SFS as a special case.

To aggregate RT-SFS information effectively in MAGDM, advanced aggregation mechanisms are required. Among these, Aczél–Alsina (AA) aggregation operators (AOs), derived from the AA $\mathfrak{t}$-norm and $\mathfrak{t}$-conorm [17], provide a flexible mathematical framework in which a parameterized Archimedean structure allows systematic adjustment of aggregation behavior and well-defined limiting properties. This flexibility makes AA aggregation suitable for modeling the aggregation preferences of different decision-makers. Building on these properties, AA aggregation has been extended from IFSs [18] to $\mathfrak{q}$-ROFSs [19], while Hussain *et al.* [20] further developed AA operations for T-SFSs.

Effective MAGDM also requires strong discrimination among alternatives, particularly when their evaluations are closely similar. To improve such discrimination, Garg *et al.* [21] introduced sine-trigonometric (ST) operational laws and aggregation operators under the PyFS environment. By applying sine-based transformations to evaluation information before aggregation, these operators can enhance the distinction between closely related assessments while preserving their relative ordering. ST operations have subsequently been extended to SFSs [22], T-SFSs [23], LDFSs [24], and Pythagorean fuzzy normal environments [25]. In the present study, the discrimination-enhancing role of the ST transformation is further examined within the proposed RT-SFAAST framework through an ablation study in Section 8.7.3.

Despite these developments, no existing study jointly integrates Aczél–Alsina aggregation and sine-trigonometric operational laws within a reliability-aware fuzzy framework that simultaneously represents MI, AbI, NMI, and their corresponding RDs. To address this gap, the present study develops Aczél–Alsina Sine-Trigonometric AOs within the proposed RT-SFS framework. The resulting operators combine the flexibility of parameterized aggregation with enhanced information discrimination, enabling reliability-aware aggregation and improved differentiation among closely related alternatives.

To accommodate different decision-making preferences in MAGDM, various aggregation strategies have been developed. Weighted averaging (WA) and weighted geometric (WG) operators incorporate the relative importance of criteria or experts, with WG providing stronger penalization of low evaluations. To model different decision attitudes through ordered aggregation, ordered weighted averaging (OWA) operators were introduced [26], while ordered weighted geometric (OWG) operators extend this principle through geometric aggregation [27]. Accordingly, this study develops Aczél–Alsina Sine-Trigonometric weighted averaging, weighted geometric, ordered weighted averaging, and ordered weighted geometric AOs within the proposed RT-SFS framework, providing a comprehensive family of reliability-aware aggregation operators for MAGDM.

To the best of our knowledge, no existing study has simultaneously integrated a reliability-aware extension of T-spherical fuzzy sets, Aczél–Alsina aggregation, and sine-trigonometric operational laws within a unified MAGDM framework. To address this gap, this paper proposes the Reliability T-Spherical Fuzzy Set (RT-SFS) framework and a family of Aczél–Alsina Sine-Trigonometric AOs, and demonstrates their applicability to the prioritization of smart waste-management interventions in Delhi, India. The main contributions of this paper are summarized as follows:

- A reliability-aware extension of the conventional T-spherical fuzzy framework, termed the RT-SFS, is proposed by incorporating independent reliability degrees into T-spherical fuzzy information, enabling the simultaneous representation of MI, AbI, NMI, and their corresponding RDs.
- Novel Aczél–Alsina Sine-Trigonometric operational laws for RT-SFS information are developed by integrating sine-trigonometric transformations with Aczél–Alsina operations, providing flexible parameterized aggregation and enhanced discrimination among closely related assessments.
- A family of Aczél–Alsina Sine-Trigonometric AOs, comprising weighted averaging, weighted geometric, ordered weighted averaging, and ordered weighted geometric operators, is established within the proposed RT-SFS framework.
- Fundamental properties of the proposed AOs, including idempotency, boundedness, monotonicity, and commutativity, are formally established.
- A reliability-aware MAGDM methodology based on the proposed AOs is formulated for prioritizing smart waste-management interventions.
- A real-world case study in Delhi, India, together with sensitivity, ablation, and comparative analyses, is conducted to evaluate the robustness, discrimination capability, and practical applicability of the proposed framework.

The remainder of this paper is organized as follows. Section 2 introduces the fundamental concepts underlying the proposed framework. Section 3 presents the RT-SFS framework, including its definition, comparison laws, and linguistic representation. Section 4 develops the Aczél–Alsina Sine-Trigonometric operational laws, while Section 5 presents the corresponding aggregation operators and their fundamental properties. The MAGDM methodology and its application to smart waste-management intervention prioritization are presented subsequently, followed by sensitivity, ablation, and comparative analyses, as well as the study's limitations. Finally, Section 9 concludes the paper and outlines directions for future research.

2. Preliminaries

This section briefly reviews the fundamental concepts and operational laws that underpin the proposed methodology.

2.1. T-Spherical Fuzzy Set

The following definitions recall the basic concepts, ranking measures, and comparison rules associated with T-spherical fuzzy sets (T-SFSs) [13].

Definition 2.1 ([13])**.** Let $\mathcal{U}$ be a universe of discourse. A T-SFS $\mathcal{P}$ on $\mathcal{U}$ is defined as:

$$\mathcal{P} = \{\langle u, \zeta_{\mathcal{P}}(u), \omega_{\mathcal{P}}(u), \upsilon_{\mathcal{P}}(u)\rangle \mid u \in \mathcal{U}\}, \tag{2.1}$$

where $\zeta_{\mathcal{P}}(u), \omega_{\mathcal{P}}(u), \upsilon_{\mathcal{P}}(u) \in [0,1]$ denote the membership information (MI), abstinence information (AbI), and non-membership information (NMI), respectively, satisfying the condition:

$$0 \leqslant \zeta_{\mathcal{P}}^{q}(u) + \omega_{\mathcal{P}}^{q}(u) + \upsilon_{\mathcal{P}}^{q}(u) \leqslant 1, \tag{2.2}$$

for $q \geqslant 1$ and every $u \in \mathcal{U}$. For convenience, a T-spherical fuzzy number (T-SFN) is denoted by $\alpha = (\zeta, \omega, \upsilon)$.

Definition 2.2 ([13])**.** For a T-SFN $\alpha = (\zeta, \omega, \upsilon)$, the score function $S(\alpha)$ and the accuracy function $A(\alpha)$ are defined as:

$$S(\alpha) = \zeta^{q} - \upsilon^{q}, \tag{2.3}$$

and

$$A(\alpha) = \zeta^{q} + \omega^{q} + \upsilon^{q}, \tag{2.4}$$

respectively, where $S(\alpha) \in [-1,1]$ and $A(\alpha) \in [0,1]$.

Definition 2.3 ([13])**.** Let α_1 and α_2 be two T-SFNs. The ranking order is determined as follows:

(i) If $S(\alpha_1) > S(\alpha_2)$, then $\alpha_1 \succ \alpha_2$.

(ii) If $S(\alpha_1) = S(\alpha_2)$ and $A(\alpha_1) > A(\alpha_2)$, then $\alpha_1 \succ \alpha_2$.

(iii) If $S(\alpha_1) = S(\alpha_2)$ and $A(\alpha_1) = A(\alpha_2)$, then $\alpha_1 \approx \alpha_2$.

2.2. AA Operational Laws

The proposed framework utilizes the Aczél–Alsina t-norm and t-conorm for information aggregation. Their definitions are recalled below.

Definition 2.4 ([17])**.** For $u, v \in [0,1]$ and $\lambda > 0$, the Aczél–Alsina t-norm T_{AA} and t-conorm S_{AA} are defined as:

$$T_{AA}(u,v) = \exp\Big(-\big((-\ln u)^{\lambda} + (-\ln v)^{\lambda}\big)^{1/\lambda}\Big), \tag{2.5}$$

and

$$S_{AA}(u,v) = 1 - \exp\Big(-\big((-\ln(1-u))^{\lambda} + (-\ln(1-v))^{\lambda}\big)^{1/\lambda}\Big). \tag{2.6}$$

3. Reliability T-Spherical Fuzzy Sets

This section introduces RT-SFS, which extends the T-SFS framework by associating independent RDs with MI, AbI, and NMI. These RDs characterize the trustworthiness of the corresponding evaluation without modifying its original meaning. Consequently, RT-SFS provides a dual-layer representation that concurrently captures expert assessments and their associated reliability within a unified framework.

3.1. Definition of Reliability T-Spherical Fuzzy Set

The RT-SFS framework characterizes uncertainty via a dual-layer approach: the first layer captures evaluation information (MI, AbI, and NMI), while the second independently models the corresponding RDs.

Definition 3.1. Let $\mathcal{U}$ be a non-empty universe of discourse. An RT-SFS $\widetilde{\mathcal{P}}$ over $\mathcal{U}$ is defined as

$$\widetilde{\mathcal{P}} = \left\{ \left\langle u, (\zeta_{\widetilde{\mathcal{P}}}(u), \omega_{\widetilde{\mathcal{P}}}(u), \upsilon_{\widetilde{\mathcal{P}}}(u)), (\delta_{\widetilde{\mathcal{P}}}(u), \eta_{\widetilde{\mathcal{P}}}(u), \beta_{\widetilde{\mathcal{P}}}(u)) \right\rangle : u \in \mathcal{U} \right\} \tag{3.1}$$

where $\zeta_{\widetilde{\mathcal{P}}}(u), \omega_{\widetilde{\mathcal{P}}}(u), \upsilon_{\widetilde{\mathcal{P}}}(u) \in [0,1]$ denote MI, AbI, and NMI, and $\delta_{\widetilde{\mathcal{P}}}(u), \eta_{\widetilde{\mathcal{P}}}(u), \beta_{\widetilde{\mathcal{P}}}(u) \in [0,1]$ denote their RDs. For a rung parameter $q \geqslant 1$, the following admissibility condition must be satisfied:

$$0 \leqslant \zeta^q_{\widetilde{\mathcal{P}}}(u) + \omega^q_{\widetilde{\mathcal{P}}}(u) + \upsilon^q_{\widetilde{\mathcal{P}}}(u) \leqslant 1, \quad \forall u \in \mathcal{U}. \tag{3.2}$$

An element of an RT-SFS is termed an RT-SFN, denoted by $\tilde{\alpha} = ((\zeta, \omega, \upsilon), (\delta, \eta, \beta))$, where $(\zeta, \omega, \upsilon)$ and (δ, η, β) are the *evaluation triplet* and *reliability triplet*, respectively.

Remark 1. Unlike the evaluation triplet $(\zeta, \omega, \upsilon)$, which must satisfy the T-spherical admissibility condition in Eq. (3.2), the reliability triplet (δ, η, β) independently represents the reliability of the corresponding evaluation components. Therefore, each reliability degree is only required to belong to $[0,1]$ without satisfying any joint T-spherical constraint. This decoupled representation enables RT-SFS to incorporate reliability information while preserving the original evaluation semantics, thereby avoiding distortion of the expert's assessment due to reliability uncertainty.

Example 3.1 (Motivation for Reliability Degrees)**.** Suppose experts E_k and E_{k+1} evaluate alternative A_i under criterion C_j with the same T-SFN $(0.8, 0.1, 0.1)$. Owing to extensive experience and sufficient supporting evidence, E_k assigns the reliability triplet $(0.9, 0.7, 0.8)$, whereas E_{k+1}, having limited experience and supporting data, assigns $(0.4, 0.3, 0.4)$. The corresponding RT-SFNs are

$$\tilde{\alpha}_k = ((0.8, 0.1, 0.1), (0.9, 0.7, 0.8)), \qquad \tilde{\alpha}_{k+1} = ((0.8, 0.1, 0.1), (0.4, 0.3, 0.4)).$$

Under the conventional T-SFS framework [13], these two assessments are indistinguishable because they possess identical evaluation triplets. In contrast, the proposed RT-SFS framework distinguishes them through their reliability triplets, enabling the aggregation operators and ranking process to explicitly account for the confidence associated with expert assessments.

Remark 2. RT-SFS generalizes several existing fuzzy models under particular parameter settings:

- If $\delta = \eta = \beta = 1$, RT-SFS reduces to the conventional T-SFS [13].
- If $\omega = \eta = 0$, it reduces to a reliability-aware q-rung orthopair fuzzy set, consistent with Sq-ROFS [16].
- If $q = 2$, $\omega = \eta = 0$, and $\delta = \beta = 1$, it reduces to the conventional Pythagorean fuzzy set [12].
- If $q = 1$, $\omega = \eta = 0$, and $\delta = \beta = 1$, it reduces to the conventional intuitionistic fuzzy set [9].

Thus, RT-SFS provides a unified reliability-aware framework that encompasses several existing fuzzy models as special cases.

3.2. Comparison Laws for Reliability T-Spherical Fuzzy Numbers

To rank RT-SFNs, the following reliability-aware score and accuracy functions are established. Unlike the traditional measure [13] in Eq. (2.3), which omits AbI and RDs, the proposed score function concurrently integrates MI, AbI, NMI, and their respective RDs to facilitate reliability-aware decision-making.

Definition 3.2. For an RT-SFN $\tilde{\alpha} = ((\zeta, \omega, \upsilon), (\delta, \eta, \beta))$, the score function $S(\tilde{\alpha})$ and accuracy function $A(\tilde{\alpha})$ are defined as:

$$S(\tilde{\alpha}) = \frac{1 + \delta\zeta^q - \eta\omega^q - \beta\upsilon^q}{2} \tag{3.3}$$

$$A(\tilde{\alpha}) = \delta\zeta^q + \eta\omega^q + \beta\upsilon^q \tag{3.4}$$

where $S(\tilde{\alpha}), A(\tilde{\alpha}) \in [0,1]$.

Definition 3.3. For any two RT-SFNs $\tilde{\alpha}_1$ and $\tilde{\alpha}_2$, the ranking order is determined as follows:

(i) If $S(\tilde{\alpha}_1) > S(\tilde{\alpha}_2)$, then $\tilde{\alpha}_1 \succ \tilde{\alpha}_2$.

(ii) If $S(\tilde{\alpha}_1) = S(\tilde{\alpha}_2)$, then:

- If $A(\tilde{\alpha}_1) > A(\tilde{\alpha}_2)$, then $\tilde{\alpha}_1 \succ \tilde{\alpha}_2$.
- If $A(\tilde{\alpha}_1) < A(\tilde{\alpha}_2)$, then $\tilde{\alpha}_1 \prec \tilde{\alpha}_2$.
- If $A(\tilde{\alpha}_1) = A(\tilde{\alpha}_2)$, then $\tilde{\alpha}_1 \sim \tilde{\alpha}_2$.

3.3. Properties of the Reliability-Aware Score and Accuracy Functions

To verify the mathematical validity of the proposed functions, the following properties are established.

Theorem 3.1. *Let $\tilde{\alpha} = ((\zeta, \omega, \upsilon), (\delta, \eta, \beta))$ be an RT-SFN. The score function $S(\tilde{\alpha})$ and accuracy function $A(\tilde{\alpha})$ satisfy the following:*

(i) ***Boundedness:*** *$0 \leqslant S(\tilde{\alpha}) \leqslant 1$ and $0 \leqslant A(\tilde{\alpha}) \leqslant 1$.*

(ii) ***Monotonicity:*** *$S(\tilde{\alpha})$ is non-decreasing with respect to MI (ζ) and its RD (δ), and non-increasing with respect to AbI (ω), NMI (υ), and their respective RDs (η, β).*

(iii) ***Reliability-free Reduction:*** *If $\delta = \eta = \beta = 1$, the functions reduce to their reliability-free forms.*

(iv) ***Reliability Impact:*** *If $\delta, \eta, \beta \to 0$, then $S(\tilde{\alpha}) \to 0.5$ and $A(\tilde{\alpha}) \to 0$.*

Proof. (i) Since $0 \leqslant \delta, \eta, \beta, \zeta, \omega, \upsilon \leqslant 1$ and $\zeta^q + \omega^q + \upsilon^q \leqslant 1$, the term $\delta\zeta^q - \eta\omega^q - \beta\upsilon^q$ is bounded in $[-1, 1]$, yielding $0 \leqslant S(\tilde{\alpha}) \leqslant 1$. Similarly, $0 \leqslant \delta\zeta^q + \eta\omega^q + \beta\upsilon^q \leqslant 1$ ensures $0 \leqslant A(\tilde{\alpha}) \leqslant 1$.

(ii) The partial derivatives satisfy: $\frac{\partial S}{\partial \zeta} = \frac{q\delta\zeta^{q-1}}{2} \geqslant 0$, $\frac{\partial S}{\partial \delta} = \frac{\zeta^q}{2} \geqslant 0$, $\frac{\partial S}{\partial \omega} = -\frac{q\eta\omega^{q-1}}{2} \leqslant 0$, $\frac{\partial S}{\partial \eta} = -\frac{\omega^q}{2} \leqslant 0$, $\frac{\partial S}{\partial \upsilon} = -\frac{q\beta\upsilon^{q-1}}{2} \leqslant 0$, and $\frac{\partial S}{\partial \beta} = -\frac{\upsilon^q}{2} \leqslant 0$. This confirms the monotonic behavior relative to the input assessment and its reliability.

(iii) Setting $\delta = \eta = \beta = 1$ gives $S(\tilde{\alpha}) = \frac{1+\zeta^q-\omega^q-\upsilon^q}{2}$ and $A(\tilde{\alpha}) = \zeta^q + \omega^q + \upsilon^q$, which correspond to the proposed score and accuracy functions without reliability information.

(iv) As $\delta, \eta, \beta \to 0$, the reliability-weighted components vanish, yielding $S(\tilde{\alpha}) \to 0.5$ and $A(\tilde{\alpha}) \to 0$, indicating a total absence of reliable information. □

3.4. Linguistic Representation of Expert Assessments

For practical decision-making, experts assess the performance of alternatives using linguistic terms and specify the reliability of each assessment through a qualitative reliability scale. These assessments are mapped to evaluation triplets $(\zeta, \omega, \upsilon)$ and reliability triplets (δ, η, β) to construct the RT-SFNs used throughout the proposed framework.

Following standard T-SFS literature [13], the rung parameter is fixed at $q = 3$. Compared with $q = 1$ and $q = 2$, choosing $q = 3$ enlarges the feasible domain, allowing experts greater flexibility to simultaneously express MI, AbI, and NMI while satisfying Eq. (3.2). The reference evaluation triplets in Table 1 are designed to preserve semantic ordering and ensure numerical discrimination, while the reliability triplets in Table 2 quantify assessment confidence.

Table 1: Performance linguistic terms and corresponding evaluation triplets ($q = 3$).

Linguistic Term	**Notation**	$(\zeta, \omega, \upsilon)$	**Performance Level**
Excellent	EX	$(0.95, 0.05, 0.05)$	Outstanding performance
Very Good	VG	$(0.85, 0.10, 0.15)$	Strong performance
Good	G	$(0.75, 0.20, 0.25)$	Above-average performance
Fair	F	$(0.60, 0.30, 0.45)$	Moderate performance
Poor	P	$(0.40, 0.40, 0.65)$	Below-average performance
Very Poor	VP	$(0.25, 0.50, 0.80)$	Unsatisfactory performance
Extremely Poor	EP	$(0.10, 0.60, 0.90)$	Extremely unsatisfactory

Table 2: Reliability linguistic terms and corresponding reliability triplets.

Reliability Level	**Notation**	(δ, η, β)	**Assessment Confidence**
Very High Reliability	VHR	$(1.00, 0.00, 0.00)$	Almost complete confidence
High Reliability	HR	$(0.85, 0.15, 0.15)$	High confidence
Moderate Reliability	MR	$(0.70, 0.30, 0.30)$	Moderate confidence
Low Reliability	LR	$(0.55, 0.45, 0.45)$	Limited confidence
Very Low Reliability	VLR	$(0.40, 0.60, 0.60)$	Highly uncertain assessment

Let $\mathcal{L} = (\ell, \mathsf{r})$ denote a linguistic assessment, where ℓ and r are selected from Tables 1 and 2, respectively. This pair is mapped to an RT-SFN, thereby simultaneously representing the qualitative evaluation and its associated reliability.

Example 3.2 (Construction of an RT-SFN)**.** Suppose expert E_k evaluates alternative A_i under criterion C_j with the linguistic assessment $(\mathsf{G}, \mathrm{HR})$. According to Tables 1 and 2, this maps to the RT-SFN:

$$\tilde{\alpha}_k = ((0.75, 0.20, 0.25), (0.85, 0.15, 0.15)).$$

If another expert assigns $(\mathsf{G}, \mathrm{MR})$, the evaluation triplet remains identical, but the reliability triplet changes to $(0.70, 0.30, 0.30)$. Consequently, the RT-SFS framework distinguishes assessments not only by their performance evaluations but also by their associated reliability levels.

4. Aczél–Alsina Sine-Trigonometric Operational Laws for Reliability T-Spherical Fuzzy Numbers

This section develops the proposed Aczél–Alsina Sine-Trigonometric (AA-ST) operational laws for RT-SFNs by integrating the sine-trigonometric transformation with the parameterized Aczél–Alsina $\mathfrak{t}$-norm and $\mathfrak{t}$-conorm, thereby enabling flexible reliability-aware aggregation while enhancing discrimination between closely related evaluations. Since the Aczél–Alsina operations act on transformed values, the evaluation components are first mapped into the sine-trigonometric domain.

Definition 4.1 (Sine-Trigonometric Transformation)**.** For an RT-SFN $\tilde{\alpha} = ((\zeta, \omega, \upsilon), (\delta, \eta, \beta))$, the corresponding ST transformed components are defined as

$$\mathcal{Z} = \sin^{\mathfrak{q}}\left(\frac{\pi}{2}\zeta\right), \quad \mathcal{W} = 1 - \sin^{\mathfrak{q}}\left(\frac{\pi}{2}\sqrt[\mathfrak{q}]{1-\omega^{\mathfrak{q}}}\right), \quad \mathcal{V} = 1 - \sin^{\mathfrak{q}}\left(\frac{\pi}{2}\sqrt[\mathfrak{q}]{1-\upsilon^{\mathfrak{q}}}\right). \tag{4.1}$$

Definition 4.2 (Inverse Sine-Trigonometric Transformation)**.** For aggregated transformed values $\mathcal{Z}, \mathcal{W}, \mathcal{V} \in [0, 1]$, the corresponding evaluation components are recovered as

$$\begin{aligned} \zeta &= \frac{2}{\pi}\arcsin\left(\mathcal{Z}^{1/\mathfrak{q}}\right), \\ \omega &= \left[1 - \left(\frac{2}{\pi}\arcsin\left((1-\mathcal{W})^{1/\mathfrak{q}}\right)\right)^{\mathfrak{q}}\right]^{1/\mathfrak{q}}, \\ \upsilon &= \left[1 - \left(\frac{2}{\pi}\arcsin\left((1-\mathcal{V})^{1/\mathfrak{q}}\right)\right)^{\mathfrak{q}}\right]^{1/\mathfrak{q}}. \end{aligned} \tag{4.2}$$

Definition 4.3 (Identity Mapping)**.** The *identity mapping* replaces the ST transformation by

$$\mathcal{Z} = \zeta^{\mathfrak{q}}, \qquad \mathcal{W} = \omega^{\mathfrak{q}}, \qquad \mathcal{V} = \upsilon^{\mathfrak{q}},$$

with inverse

$$\zeta = \mathcal{Z}^{1/\mathfrak{q}}, \qquad \omega = \mathcal{W}^{1/\mathfrak{q}}, \qquad \upsilon = \mathcal{V}^{1/\mathfrak{q}}.$$

Only the evaluation triplet $(\zeta, \omega, \upsilon)$ is transformed by the ST mapping, whereas the reliability triplet (δ, η, β) is aggregated directly using the Aczél–Alsina $\mathfrak{t}$-norm and $\mathfrak{t}$-conorm. This design enhances discrimination among evaluation assessments while preserving the interpretation of (δ, η, β) as reliability information, which is not subject to the T-spherical admissibility constraint.

Definition 4.4. Let $\tilde{\alpha}_1$ and $\tilde{\alpha}_2$ be two RT-SFNs with corresponding ST-transformed components $\mathcal{Z}$, $\mathcal{W}$, and $\mathcal{V}$ defined in Definition 4.1. Let $\lambda > 0$ be the Aczél–Alsina parameter, $\kappa > 0$ be a scalar, and $q \geqslant 1$ be the rung parameter. Then, the AA-ST operational laws are:

(i) **Addition ($\oplus$):**

$$\tilde{\alpha}_1 \oplus \tilde{\alpha}_2 = \left\langle \begin{pmatrix} \frac{2}{\pi}\arcsin\left[\left(1-\exp\left(-\left(\sum_{j=1}^{2}(-\ln(1-\mathcal{Z}_j))^{\lambda}\right)^{1/\lambda}\right)\right)^{1/q}\right], \\ \left[1-\left(\frac{2}{\pi}\arcsin\left[\left(1-\exp\left(-\left(\sum_{j=1}^{2}(-\ln \mathcal{W}_j)^{\lambda}\right)^{1/\lambda}\right)\right)^{1/q}\right]\right)^{q}\right]^{1/q}, \\ \left[1-\left(\frac{2}{\pi}\arcsin\left[\left(1-\exp\left(-\left(\sum_{j=1}^{2}(-\ln \mathcal{V}_j)^{\lambda}\right)^{1/\lambda}\right)\right)^{1/q}\right]\right)^{q}\right]^{1/q} \end{pmatrix}, \begin{pmatrix} 1-\exp\left(-\left(\sum_{j=1}^{2}(-\ln(1-\delta_j))^{\lambda}\right)^{1/\lambda}\right), \\ \exp\left(-\left(\sum_{j=1}^{2}(-\ln \eta_j)^{\lambda}\right)^{1/\lambda}\right), \\ \exp\left(-\left(\sum_{j=1}^{2}(-\ln \beta_j)^{\lambda}\right)^{1/\lambda}\right) \end{pmatrix} \right\rangle$$

(ii) **Multiplication ($\otimes$):**

$$\tilde{\alpha}_1 \otimes \tilde{\alpha}_2 = \left\langle \begin{pmatrix} \frac{2}{\pi}\arcsin\left[\left(\exp\left(-\left(\sum_{j=1}^{2}(-\ln \mathcal{Z}_j)^{\lambda}\right)^{1/\lambda}\right)\right)^{1/q}\right], \\ \left[1-\left(\frac{2}{\pi}\arcsin\left[\left(\exp\left(-\left(\sum_{j=1}^{2}(-\ln(1-\mathcal{W}_j))^{\lambda}\right)^{1/\lambda}\right)\right)^{1/q}\right]\right)^{q}\right]^{1/q}, \\ \left[1-\left(\frac{2}{\pi}\arcsin\left[\left(\exp\left(-\left(\sum_{j=1}^{2}(-\ln(1-\mathcal{V}_j))^{\lambda}\right)^{1/\lambda}\right)\right)^{1/q}\right]\right)^{q}\right]^{1/q} \end{pmatrix}, \begin{pmatrix} \exp\left(-\left(\sum_{j=1}^{2}(-\ln \delta_j)^{\lambda}\right)^{1/\lambda}\right), \\ 1-\exp\left(-\left(\sum_{j=1}^{2}(-\ln(1-\eta_j))^{\lambda}\right)^{1/\lambda}\right), \\ 1-\exp\left(-\left(\sum_{j=1}^{2}(-\ln(1-\beta_j))^{\lambda}\right)^{1/\lambda}\right) \end{pmatrix} \right\rangle$$

(iii) **Scalar Multiplication ($\kappa\tilde{\alpha}$):**

$$\kappa\tilde{\alpha} = \left\langle \begin{pmatrix} \frac{2}{\pi}\arcsin\left[\left(1-\exp\left(-\left(\kappa(-\ln(1-\mathcal{Z}))^{\lambda}\right)^{1/\lambda}\right)\right)^{1/q}\right], \\ \left[1-\left(\frac{2}{\pi}\arcsin\left[\left(1-\exp\left(-\left(\kappa(-\ln \mathcal{W})^{\lambda}\right)^{1/\lambda}\right)\right)^{1/q}\right]\right)^{q}\right]^{1/q}, \\ \left[1-\left(\frac{2}{\pi}\arcsin\left[\left(1-\exp\left(-\left(\kappa(-\ln \mathcal{V})^{\lambda}\right)^{1/\lambda}\right)\right)^{1/q}\right]\right)^{q}\right]^{1/q} \end{pmatrix}, \begin{pmatrix} 1-\exp\left(-\left(\kappa(-\ln(1-\delta))^{\lambda}\right)^{1/\lambda}\right), \\ \exp\left(-\left(\kappa(-\ln \eta)^{\lambda}\right)^{1/\lambda}\right), \\ \exp\left(-\left(\kappa(-\ln \beta)^{\lambda}\right)^{1/\lambda}\right) \end{pmatrix} \right\rangle$$

(iv) **Power Operation ($\tilde{\alpha}^{\kappa}$):**

$$\tilde{\alpha}^{\kappa} = \begin{pmatrix} \begin{pmatrix} \frac{2}{\pi}\arcsin\left[\left(\exp\left(-\left(\kappa(-\ln \mathcal{Z})^{\lambda}\right)^{1/\lambda}\right)\right)^{1/q}\right], \\ \left[1-\left(\frac{2}{\pi}\arcsin\left[\left(\exp\left(-\left(\kappa(-\ln(1-\mathcal{W}))^{\lambda}\right)^{1/\lambda}\right)\right)^{1/q}\right]\right)^{q}\right]^{1/q}, \\ \left[1-\left(\frac{2}{\pi}\arcsin\left[\left(\exp\left(-\left(\kappa(-\ln(1-\mathcal{V}))^{\lambda}\right)^{1/\lambda}\right)\right)^{1/q}\right]\right)^{q}\right]^{1/q} \end{pmatrix} \\ \begin{pmatrix} \exp\left(-\left(\kappa(-\ln \delta)^{\lambda}\right)^{1/\lambda}\right), \\ 1-\exp\left(-\left(\kappa(-\ln(1-\eta))^{\lambda}\right)^{1/\lambda}\right), \\ 1-\exp\left(-\left(\kappa(-\ln(1-\beta))^{\lambda}\right)^{1/\lambda}\right) \end{pmatrix} \end{pmatrix}$$

5. Reliability T-Spherical Fuzzy Aczél–Alsina Sine-Trigonometric Aggregation Operators

This section develops a family of RT-SFAAST AOs for aggregating RT-SFNs, comprising WA, WG, OWA, and OWG operators that integrate the AA aggregation mechanism with the ST transformation while incorporating reliability information from expert assessments. Fundamental properties of the proposed AOs, including component-wise boundedness, idempotency, monotonicity, and boundedness, are also established.

5.1. Reliability T-Spherical Fuzzy Aczél–Alsina Sine-Trigonometric Weighted Averaging Operator

The Reliability T-Spherical Fuzzy Aczél–Alsina Sine-Trigonometric Weighted Averaging (RT-SFAASTWA) operator aggregates RT-SFNs by combining the AA-ST scalar multiplication and AA-ST addition operations under a predefined weight vector (Definition 4.4), providing a reliability-aware weighted averaging mechanism within the proposed RT-SFS framework. The fundamental properties of the proposed RT-SFAASTWA operator, namely component-wise boundedness, idempotency, monotonicity, and boundedness, are established subsequently.

Definition 5.1. Let $\tilde{\alpha}_j = ((\zeta_j, \omega_j, \upsilon_j), (\delta_j, \eta_j, \beta_j))$ $(j = 1, 2, \ldots, n)$ be a collection of RT-SFNs with corresponding ST-transformed components $\mathcal{Z}_j$, $\mathcal{W}_j$, and $\mathcal{V}_j$ defined in Definition 4.1. Let $\lambda > 0$ be the Aczél–Alsina parameter, $q \geqslant 1$ be the rung parameter, and let $W = (w_1, w_2, \ldots, w_n)^{\mathsf{T}}$ be a weight vector satisfying $w_j \geqslant 0$ and $\sum_{j=1}^{n} w_j = 1$. Then, the RT-SFAASTWA operator is defined by

$$\begin{aligned} &\text{RT-SFAASTWA}(\tilde{\alpha}_1, \ldots, \tilde{\alpha}_n) = \bigoplus_{j=1}^{n} w_j \tilde{\alpha}_j \\ &= \begin{pmatrix} \begin{pmatrix} \frac{2}{\pi}\arcsin\left[\left(1-\exp\left(-\left(\sum_{j=1}^{n} w_j(-\ln(1-\mathcal{Z}_j))^{\lambda}\right)^{1/\lambda}\right)\right)^{1/q}\right], \\ \left[1-\left(\frac{2}{\pi}\arcsin\left[\left(1-\exp\left(-\left(\sum_{j=1}^{n} w_j(-\ln \mathcal{W}_j)^{\lambda}\right)^{1/\lambda}\right)\right)^{1/q}\right]\right)^{q}\right]^{1/q}, \\ \left[1-\left(\frac{2}{\pi}\arcsin\left[\left(1-\exp\left(-\left(\sum_{j=1}^{n} w_j(-\ln \mathcal{V}_j)^{\lambda}\right)^{1/\lambda}\right)\right)^{1/q}\right]\right)^{q}\right]^{1/q} \end{pmatrix} \\ \begin{pmatrix} 1-\exp\left(-\left(\sum_{j=1}^{n} w_j(-\ln(1-\delta_j))^{\lambda}\right)^{1/\lambda}\right), \\ \exp\left(-\left(\sum_{j=1}^{n} w_j(-\ln \eta_j)^{\lambda}\right)^{1/\lambda}\right), \\ \exp\left(-\left(\sum_{j=1}^{n} w_j(-\ln \beta_j)^{\lambda}\right)^{1/\lambda}\right) \end{pmatrix} \end{pmatrix} \end{aligned}$$

That is, each RT-SFN is first weighted using the AA-ST scalar multiplication operation with weight w_j (Definition 4.4 (iii)), and the resulting weighted RT-SFNs are subsequently aggregated using the AA-ST addition operation (Definition 4.4 (i)).

Remark 3 (Special Cases)**.** The proposed RT-SFAASTWA operator (Definition 5.1) reduces to several existing aggregation models as special cases.

(i) At $\lambda = 1$, the Aczél–Alsina t-norm and t-conorm reduce to the algebraic product and algebraic sum, respectively, and the RT-SFAASTWA operator reduces to the reliability T-spherical fuzzy algebraic sine-trigonometric weighted averaging operator.

(ii) Replacing the sine-trigonometric transformation with the identity mapping (Definition 4.3) yields the reliability T-spherical fuzzy Aczél–Alsina weighted averaging operator.

(iii) Setting $\delta = \eta = \beta = 1$ reduces the operator to its reliability-free case, namely the T-spherical fuzzy Aczél–Alsina sine-trigonometric weighted averaging operator.

(iv) Further setting $q = 2$ and $q = 1$ (with $\delta = \eta = \beta = 1$) yields the corresponding spherical- and picture-fuzzy Aczél–Alsina sine-trigonometric weighted averaging operators, respectively.

Theorem 5.1 (Component-wise Boundedness). *For any collection of RT-SFNs $\tilde{\alpha}_j = ((\zeta_j, \omega_j, \upsilon_j), (\delta_j, \eta_j, \beta_j))$ $(j = 1, 2, \ldots, n)$ and any weight vector $W = (w_1, \ldots, w_n)^T$ satisfying $w_j \geqslant 0$ and $\sum_{j=1}^{n} w_j = 1$, let the aggregated result be $\tilde{\alpha}_{agg} = \text{RT-SFAASTWA}(\tilde{\alpha}_1, \ldots, \tilde{\alpha}_n)$. Then:*

(i) Every component of the evaluation triplet $(\zeta, \omega, \upsilon)$ belongs to the unit interval $[0, 1]$.

(ii) Every component of the reliability triplet (δ, η, β) belongs to the unit interval $[0, 1]$.

Proof. (i) We prove the boundedness for the membership component ζ. Let $f(t) = (-\ln(1-t))^\lambda$ denote the generator function associated with the Aczél–Alsina t-conorm. By Definition 5.1, the aggregated ST-transformed membership is given by:

$$\mathcal{Z}_{agg} = 1 - \exp\left(-\left(\sum_{j=1}^{n} w_j(-\ln(1-\mathcal{Z}_j))^\lambda\right)^{1/\lambda}\right)$$

Since $\zeta_j \in [0, 1]$, the ST-transformation $\mathcal{Z}_j = \sin^q(\frac{\pi}{2}\zeta_j)$ ensures $\mathcal{Z}_j \in [0, 1]$. Consequently, $1 - \mathcal{Z}_j \in [0, 1]$, and the term $(-\ln(1-\mathcal{Z}_j))^\lambda \in [0, \infty)$. Given $w_j \geqslant 0$ and $\sum w_j = 1$, the weighted sum $\sum_{j=1}^{n} w_j(-\ln(1-\mathcal{Z}_j))^\lambda$ is non-negative. Let $X = \left(\sum_{j=1}^{n} w_j(-\ln(1-\mathcal{Z}_j))^\lambda\right)^{1/\lambda}$. As $X \geqslant 0$, it follows that $\exp(-X) \in (0, 1]$, and thus $1 - \exp(-X) \in [0, 1)$. Therefore, $\mathcal{Z}_{agg} \in [0, 1]$. The inverse ST-transformation

$$\zeta = \frac{2}{\pi}\arcsin(\mathcal{Z}_{agg}^{1/q})$$

maps the interval $[0, 1]$ into $[0, 1]$, confirming that $\zeta \in [0, 1]$.

For the abstinence and non-membership components, the operator utilizes the Aczél–Alsina t-norm generator $g(t) = (-\ln t)^\lambda$. Since $\mathcal{W}_j, \mathcal{V}_j \in [0, 1]$, the non-negative weighted sum of their generators ensures the inverse generator $g^{-1}(x) = \exp(-x^{1/\lambda})$ maps back to $[0, 1]$. The subsequent inverse ST-transformation maps the resulting values from $[0, 1]$ into $[0, 1]$, and hence $\omega, \upsilon \in [0, 1]$.

(ii) The reliability components (δ, η, β) are aggregated directly using the Aczél–Alsina t-conorm and t-norm. Since the input reliability degrees $\delta_j, \eta_j, \beta_j$ belong to $[0, 1]$, and the interval $[0, 1]$ is closed under the strict Archimedean operations of the Aczél–Alsina family, it follows that $\delta, \eta, \beta \in [0, 1]$. □

Theorem 5.2 (Idempotency). *Let $\tilde{\alpha}_j = ((\zeta_j, \omega_j, \upsilon_j), (\delta_j, \eta_j, \beta_j))$ $(j = 1, 2, \ldots, n)$ be a collection of RT-SFNs. If all RT-SFNs are identical, such that $\tilde{\alpha}_j = \tilde{\alpha} = ((\zeta, \omega, \upsilon), (\delta, \eta, \beta))$ for all j, then:*

$$\text{RT-SFAASTWA}(\tilde{\alpha}_1, \ldots, \tilde{\alpha}_n) = \tilde{\alpha}.$$

Proof. Since $\tilde{\alpha}_j = \tilde{\alpha}$ for all j, the transformed evaluation components are constant: $\mathcal{Z}_j = \mathcal{Z}$, $\mathcal{W}_j = \mathcal{W}$, and $\mathcal{V}_j = \mathcal{V}$ for all j.

For the membership component ζ_{agg}, we apply Definition 5.1. Given $\sum_{j=1}^{n} w_j = 1$:

$$\begin{aligned}
\zeta_{agg} &= \frac{2}{\pi}\arcsin\left[\left(1 - \exp\left(-\left(\sum_{j=1}^{n} w_j(-\ln(1-\mathcal{Z}))^\lambda\right)^{1/\lambda}\right)\right)^{1/q}\right] \\
&= \frac{2}{\pi}\arcsin\left[\left(1 - \exp\left(-[(-\ln(1-\mathcal{Z}))^\lambda]^{1/\lambda}\right)\right)^{1/q}\right] \\
&= \frac{2}{\pi}\arcsin\left[(1-(1-\mathcal{Z}))^{1/q}\right] = \frac{2}{\pi}\arcsin(\mathcal{Z}^{1/q}).
\end{aligned}$$

Substituting the ST-transformation $\mathcal{Z} = \sin^q(\frac{\pi}{2}\zeta)$:

$$\zeta_{agg} = \frac{2}{\pi}\arcsin\left(\sin\left(\frac{\pi}{2}\zeta\right)\right).$$

Since $\zeta \in [0,1]$, the argument $\frac{\pi}{2}\zeta$ lies in $[0, \frac{\pi}{2}]$, where $\arcsin(\sin x) = x$ holds. Thus, $\zeta_{agg} = \zeta$.

For the abstinence component ω_{agg}, substituting the identical values yields:

$$\begin{aligned}\omega_{agg} &= \left[1 - \left(\frac{2}{\pi}\arcsin\left[\left(1 - \exp\left(-\left(\sum_{j=1}^{n} w_j(-\ln \mathcal{W})^\lambda\right)^{1/\lambda}\right)\right)^{1/q}\right]\right)^q\right]^{1/q} \\ &= \left[1 - \left(\frac{2}{\pi}\arcsin\left[(1-\mathcal{W})^{1/q}\right]\right)^q\right]^{1/q}.\end{aligned}$$

Substituting the ST-transformation $1 - \mathcal{W} = \sin^q\left(\frac{\pi}{2}\sqrt[q]{1-\omega^q}\right)$:

$$\omega_{agg} = \left[1 - \left(\frac{2}{\pi}\arcsin\left(\sin\left(\frac{\pi}{2}\sqrt[q]{1-\omega^q}\right)\right)\right)^q\right]^{1/q}.$$

As $0 \leqslant \sqrt[q]{1-\omega^q} \leqslant 1$, the argument of the sine function is restricted to $[0, \frac{\pi}{2}]$. Therefore:

$$\omega_{agg} = \left[1 - \left(\sqrt[q]{1-\omega^q}\right)^q\right]^{1/q} = [1 - (1-\omega^q)]^{1/q} = \omega.$$

The proof for the non-membership component $\upsilon_{agg} = \upsilon$ follows analogously.

For the reliability components, we consider the membership reliability degree δ_{agg}:

$$\delta_{agg} = 1 - \exp\left(-\left(\sum_{j=1}^{n} w_j(-\ln(1-\delta))^\lambda\right)^{1/\lambda}\right) = 1 - (1-\delta) = \delta.$$

The proofs for $\eta_{agg} = \eta$ and $\beta_{agg} = \beta$ follow by similar algebraic substitution using the Aczél–Alsina t-norm. Consequently, RT-SFAASTWA$(\tilde{\alpha}_1, \ldots, \tilde{\alpha}_n) = \tilde{\alpha}$. □

Theorem 5.3 (Monotonicity)**.** *Let* $\tilde{\alpha}_j = ((\zeta_j, \omega_j, \upsilon_j), (\delta_j, \eta_j, \beta_j))$ *and* $\tilde{\alpha}_j^* = \left((\zeta_j^*, \omega_j^*, \upsilon_j^*), (\delta_j^*, \eta_j^*, \beta_j^*)\right)$ *($j = 1, 2, \ldots, n$) be two collections of RT-SFNs such that* $\zeta_j \leqslant \zeta_j^*$, $\omega_j \geqslant \omega_j^*$, $\upsilon_j \geqslant \upsilon_j^*$, $\delta_j \leqslant \delta_j^*$, $\eta_j \geqslant \eta_j^*$, *and* $\beta_j \geqslant \beta_j^*$ *for all* j. *Then:*

$$\text{RT-SFAASTWA}(\tilde{\alpha}_1, \ldots, \tilde{\alpha}_n) \leqslant \text{RT-SFAASTWA}(\tilde{\alpha}_1^*, \ldots, \tilde{\alpha}_n^*).$$

Proof. Let $\tilde{\alpha}$ and $\tilde{\alpha}^*$ be the aggregated results for the two collections. By Theorem 3.1 and Definition 3.3, it is sufficient to prove that the operator preserves the component-wise ordering: $\zeta \leqslant \zeta^*$, $\omega \geqslant \omega^*$, $\upsilon \geqslant \upsilon^*$, $\delta \leqslant \delta^*$, $\eta \geqslant \eta^*$, and $\beta \geqslant \beta^*$.

For the membership component, let $f(t) = (-\ln(1-t))^\lambda$. Since both the ST-transformation $\mathcal{Z}_j = \sin^q(\frac{\pi}{2}\zeta_j)$ and the generator f are strictly increasing on $[0,1]$, $\zeta_j \leqslant \zeta_j^*$ implies $\mathcal{Z}_j \leqslant \mathcal{Z}_j^*$. The aggregated membership is:

$$\zeta = \frac{2}{\pi}\arcsin\left(\left[f^{-1}\left(\sum_{j=1}^{n} w_j f(\mathcal{Z}_j)\right)\right]^{1/q}\right).$$

Since f, f^{-1}, $x^{1/q}$, arcsin, and the weighted sum are all non-decreasing on their respective domains, the composition preserves the ordering, yielding $\zeta \leqslant \zeta^*$.

For the abstinence component, since the ST-transformation $\mathcal{W}_j = 1 - \sin^q\left(\frac{\pi}{2}\sqrt[q]{1-\omega_j^q}\right)$ is a composition of monotone functions on $[0,1]$, it is strictly increasing with respect to ω_j. Hence, $\omega_j \geqslant \omega_j^*$ implies $\mathcal{W}_j \geqslant \mathcal{W}_j^*$. The aggregated abstinence is obtained via the Aczél–Alsina t-norm generator $g(t) = (-\ln t)^\lambda$. Since g is strictly decreasing, we have $g(\mathcal{W}_j) \leqslant g(\mathcal{W}_j^*)$. Taking weighted sums preserves the inequality:

$$\sum_{j=1}^{n} w_j g(\mathcal{W}_j) \leqslant \sum_{j=1}^{n} w_j g(\mathcal{W}_j^*).$$

Since the inverse generator $g^{-1}(x) = \exp(-x^{1/\lambda})$ is also strictly decreasing, it reverses the inequality:

$$g^{-1}\left(\sum_{j=1}^{n} w_j g(\mathcal{W}_j)\right) \geqslant g^{-1}\left(\sum_{j=1}^{n} w_j g(\mathcal{W}_j^*)\right).$$

Applying the inverse ST-transformation, which preserves the ordering because the ST-transformation is strictly increasing, yields $\omega \geqslant \omega^*$. The proof for the non-membership component $\upsilon \geqslant \upsilon^*$ is analogous.

For the reliability components, δ, η, and β are aggregated via standard Aczél–Alsina weighted averaging and geometric operations. By the fundamental monotonicity property of triangular norms and conorms, the ordering of the input reliability degrees is preserved, resulting in $\delta \leqslant \delta^*$, $\eta \geqslant \eta^*$, and $\beta \geqslant \beta^*$.

As all components satisfy the required conditions relative to the score function, it follows that $S(\tilde{\alpha}) \leqslant S(\tilde{\alpha}^*)$, confirming the monotonicity of the operator. □

Theorem 5.4 (Boundedness). *Let $\tilde{\alpha}_{\min} = \min\{\tilde{\alpha}_1, \ldots, \tilde{\alpha}_n\}$ and $\tilde{\alpha}_{\max} = \max\{\tilde{\alpha}_1, \ldots, \tilde{\alpha}_n\}$ be the lower and upper bounds of a collection of RT-SFNs with respect to the ordering defined in Definition 3.3. Then:*

$$\tilde{\alpha}_{\min} \leqslant \text{RT-SFAASTWA}(\tilde{\alpha}_1, \ldots, \tilde{\alpha}_n) \leqslant \tilde{\alpha}_{\max}.$$

Proof. Let $\tilde{\alpha}_j = ((\zeta_j, \omega_j, \upsilon_j), (\delta_j, \eta_j, \beta_j))$ for $j = 1, 2, \ldots, n$. By the definition of the minimum and maximum elements in a collection, the following inequalities hold for all j:

$$\tilde{\alpha}_{\min} \leqslant \tilde{\alpha}_j \leqslant \tilde{\alpha}_{\max}.$$

Let $W = (w_1, w_2, \ldots, w_n)^T$ be a weight vector such that $w_j \geqslant 0$ and $\sum_{j=1}^{n} w_j = 1$. Since the RT-SFAASTWA operator satisfies the monotonicity property (Theorem 5.3), applying the operator to the terms of the inequality yields:

$$\text{RT-SFAASTWA}(\tilde{\alpha}_{\min}, \ldots, \tilde{\alpha}_{\min}) \leqslant \text{RT-SFAASTWA}(\tilde{\alpha}_1, \ldots, \tilde{\alpha}_n) \leqslant \text{RT-SFAASTWA}(\tilde{\alpha}_{\max}, \ldots, \tilde{\alpha}_{\max}).$$

Furthermore, since the RT-SFAASTWA operator satisfies the idempotency property (Theorem 5.2), we have:

$$\text{RT-SFAASTWA}(\tilde{\alpha}_{\min}, \ldots, \tilde{\alpha}_{\min}) = \tilde{\alpha}_{\min}$$

and

$$\text{RT-SFAASTWA}(\tilde{\alpha}_{\max}, \ldots, \tilde{\alpha}_{\max}) = \tilde{\alpha}_{\max}.$$

Substituting these identities into the monotonicity inequality results in:

$$\tilde{\alpha}_{\min} \leqslant \text{RT-SFAASTWA}(\tilde{\alpha}_1, \ldots, \tilde{\alpha}_n) \leqslant \tilde{\alpha}_{\max}.$$

Thus, the aggregated RT-SFN is bounded between the minimum and maximum of the input RT-SFNs, which completes the proof. □

5.2. Reliability T-Spherical Fuzzy Aczél–Alsina Sine-Trigonometric Weighted Geometric Operator

The Reliability T-Spherical Fuzzy Aczél–Alsina Sine-Trigonometric Weighted Geometric (RT-SFAASTWG) operator aggregates RT-SFNs by combining the AA-ST power and AA-ST multiplication operations under a predefined weight vector (Definition 4.4), thereby providing a reliability-aware weighted geometric aggregation mechanism within the proposed RT-SFS framework. Its fundamental properties follow analogously to those of the RT-SFAASTWA operator, and the corresponding proofs are therefore omitted.

Definition 5.2. Let $\tilde{\alpha}_j = ((\zeta_j, \omega_j, \upsilon_j), (\delta_j, \eta_j, \beta_j))$ $(j = 1, 2, \ldots, n)$ be a collection of RT-SFNs with corresponding ST-transformed components $\mathcal{Z}_j$, $\mathcal{W}_j$, and $\mathcal{V}_j$ defined in Definition 4.1. Let $\lambda > 0$ be the Aczél–Alsina parameter, $q \geqslant 1$ be the rung parameter, and let $W = (w_1, w_2, \ldots, w_n)^T$ be a weight vector

satisfying $w_j \geqslant 0$ and $\sum_{j=1}^{n} w_j = 1$. Then, the RT-SFAASTWG operator is defined by:

$$\text{RT-SFAASTWG}(\tilde{\alpha}_1, \ldots, \tilde{\alpha}_n) = \bigotimes_{j=1}^{n} (\tilde{\alpha}_j)^{w_j}$$

$$= \left(\begin{array}{l} \left(\begin{array}{l} \frac{2}{\pi} \arcsin \left[\left(\exp\left(- \left(\sum_{j=1}^{n} w_j (-\ln \mathcal{Z}_j)^{\lambda} \right)^{1/\lambda} \right) \right)^{1/q} \right], \\ \left[1 - \left(\frac{2}{\pi} \arcsin \left[\left(\exp\left(- \left(\sum_{j=1}^{n} w_j (-\ln(1-\mathcal{W}_j))^{\lambda} \right)^{1/\lambda} \right) \right)^{1/q} \right] \right)^{q} \right]^{1/q}, \\ \left[1 - \left(\frac{2}{\pi} \arcsin \left[\left(\exp\left(- \left(\sum_{j=1}^{n} w_j (-\ln(1-\mathcal{V}_j))^{\lambda} \right)^{1/\lambda} \right) \right)^{1/q} \right] \right)^{q} \right]^{1/q} \end{array} \right) \\ \left(\begin{array}{l} \exp\left(- \left(\sum_{j=1}^{n} w_j (-\ln \delta_j)^{\lambda} \right)^{1/\lambda} \right), \\ 1 - \exp\left(- \left(\sum_{j=1}^{n} w_j (-\ln(1-\eta_j))^{\lambda} \right)^{1/\lambda} \right), \\ 1 - \exp\left(- \left(\sum_{j=1}^{n} w_j (-\ln(1-\beta_j))^{\lambda} \right)^{1/\lambda} \right) \end{array} \right) \end{array} \right)$$

That is, each RT-SFN is first weighted using the AA-ST power operation with weight w_j (Definition 4.4 (iv)), and the resulting weighted RT-SFNs are subsequently aggregated using the AA-ST multiplication operation (Definition 4.4 (ii)).

5.3. Reliability T-Spherical Fuzzy Aczél–Alsina Sine-Trigonometric Ordered Weighted Averaging Operator

The Reliability T-Spherical Fuzzy Aczél–Alsina Sine-Trigonometric Ordered Weighted Averaging (RT-SFAASTOWA) operator extends the RT-SFAASTWA operator (Definition 5.1) by incorporating an ordering mechanism based on the reliability-aware score function (Definition 3.2). Specifically, the input RT-SFNs are first arranged in descending order according to the reliability-aware score function and are subsequently aggregated using the AA-ST addition operation under the corresponding ordered weight vector. Its fundamental properties follow analogously to those of the RT-SFAASTWA operator, and the corresponding proofs are therefore omitted.

Definition 5.3. Let $\tilde{\alpha}_j = ((\zeta_j, \omega_j, \upsilon_j), (\delta_j, \eta_j, \beta_j))$ $(j = 1, 2, \ldots, n)$ be a collection of RT-SFNs with corresponding ST-transformed components $\mathcal{Z}_j$, $\mathcal{W}_j$, and $\mathcal{V}_j$ defined in Definition 4.1. Let $\lambda > 0$ be the Aczél–Alsina parameter, $q \geqslant 1$ be the rung parameter, and let $W = (w_1, w_2, \ldots, w_n)^{\mathsf{T}}$ be an ordered weight vector satisfying $w_j \geqslant 0$ and $\sum_{j=1}^{n} w_j = 1$. Then, the RT-SFAASTOWA operator is defined as:

$$\text{RT-SFAASTOWA}(\tilde{\alpha}_1, \ldots, \tilde{\alpha}_n) = \bigoplus_{j=1}^{n} w_j \tilde{\alpha}_{\sigma(j)}$$

$$= \left(\begin{array}{l} \left(\begin{array}{l} \frac{2}{\pi} \arcsin \left[\left(1 - \exp\left(- \left(\sum_{j=1}^{n} w_j (-\ln(1-\mathcal{Z}_{\sigma(j)}))^{\lambda} \right)^{1/\lambda} \right) \right)^{1/q} \right], \\ \left[1 - \left(\frac{2}{\pi} \arcsin \left[\left(1 - \exp\left(- \left(\sum_{j=1}^{n} w_j (-\ln \mathcal{W}_{\sigma(j)})^{\lambda} \right)^{1/\lambda} \right) \right)^{1/q} \right] \right)^{q} \right]^{1/q}, \\ \left[1 - \left(\frac{2}{\pi} \arcsin \left[\left(1 - \exp\left(- \left(\sum_{j=1}^{n} w_j (-\ln \mathcal{V}_{\sigma(j)})^{\lambda} \right)^{1/\lambda} \right) \right)^{1/q} \right] \right)^{q} \right]^{1/q} \end{array} \right) \\ \left(\begin{array}{l} 1 - \exp\left(- \left(\sum_{j=1}^{n} w_j (-\ln(1-\delta_{\sigma(j)}))^{\lambda} \right)^{1/\lambda} \right), \\ \exp\left(- \left(\sum_{j=1}^{n} w_j (-\ln \eta_{\sigma(j)})^{\lambda} \right)^{1/\lambda} \right), \\ \exp\left(- \left(\sum_{j=1}^{n} w_j (-\ln \beta_{\sigma(j)})^{\lambda} \right)^{1/\lambda} \right) \end{array} \right) \end{array} \right)$$

where σ is a permutation of $\{1, 2, \ldots, n\}$ satisfying $S(\tilde{\alpha}_{\sigma(1)}) \geqslant S(\tilde{\alpha}_{\sigma(2)}) \geqslant \cdots \geqslant S(\tilde{\alpha}_{\sigma(n)})$, and $S(\cdot)$ is the reliability-aware score function defined in Definition 3.2. That is, the input RT-SFNs are first arranged in descending order according to the reliability-aware score function, and the ordered RT-SFNs are subsequently aggregated using the AA-ST addition operation under the ordered weight vector.

5.4. Reliability T-Spherical Fuzzy Aczél–Alsina Sine-Trigonometric Ordered Weighted Geometric Operator

The Reliability T-Spherical Fuzzy Aczél–Alsina Sine-Trigonometric Ordered Weighted Geometric (RT-SFAASTOWG) operator extends the RT-SFAASTWG operator (Definition 5.2) by incorporating an ordering mechanism based on the reliability-aware score function (Definition 3.2). Specifically, the input RT-SFNs are first arranged in descending order according to the reliability-aware score function and are subsequently aggregated using the AA-ST multiplication operation under the corresponding ordered weight vector. Its fundamental properties follow analogously to those of the RT-SFAASTWG operator, and the corresponding proofs are therefore omitted.

Definition 5.4. Let $\tilde{\alpha}_j = ((\zeta_j, \omega_j, \upsilon_j), (\delta_j, \eta_j, \beta_j))$ $(j = 1, 2, \ldots, n)$ be a collection of RT-SFNs with corresponding ST-transformed components $\mathcal{Z}_j$, $\mathcal{W}_j$, and $\mathcal{V}_j$ defined in Definition 4.1. Let $\lambda > 0$ be the Aczél–Alsina parameter, $q \geqslant 1$ be the rung parameter, and let $W = (w_1, w_2, \ldots, w_n)^T$ be an ordered weight vector satisfying $w_j \geqslant 0$ and $\sum_{j=1}^{n} w_j = 1$. Then, the RT-SFAASTOWG operator is defined as:

$$\text{RT-SFAASTOWG}(\tilde{\alpha}_1, \ldots, \tilde{\alpha}_n) = \bigotimes_{j=1}^{n} (\tilde{\alpha}_{\sigma(j)})^{w_j}$$

$$= \left(\begin{array}{c} \left(\begin{array}{l} \frac{2}{\pi} \arcsin \left[\left(\exp\left(- \left(\sum_{j=1}^{n} w_j (-\ln \mathcal{Z}_{\sigma(j)})^{\lambda} \right)^{1/\lambda} \right) \right)^{1/q} \right], \\ \left[1 - \left(\frac{2}{\pi} \arcsin \left[\left(\exp\left(- \left(\sum_{j=1}^{n} w_j (-\ln(1 - \mathcal{W}_{\sigma(j)}))^{\lambda} \right)^{1/\lambda} \right) \right)^{1/q} \right] \right)^{q} \right]^{1/q}, \\ \left[1 - \left(\frac{2}{\pi} \arcsin \left[\left(\exp\left(- \left(\sum_{j=1}^{n} w_j (-\ln(1 - \mathcal{V}_{\sigma(j)}))^{\lambda} \right)^{1/\lambda} \right) \right)^{1/q} \right] \right)^{q} \right]^{1/q} \end{array} \right) \\ \left(\begin{array}{l} \exp\left(- \left(\sum_{j=1}^{n} w_j (-\ln \delta_{\sigma(j)})^{\lambda} \right)^{1/\lambda} \right), \\ 1 - \exp\left(- \left(\sum_{j=1}^{n} w_j (-\ln(1 - \eta_{\sigma(j)}))^{\lambda} \right)^{1/\lambda} \right), \\ 1 - \exp\left(- \left(\sum_{j=1}^{n} w_j (-\ln(1 - \beta_{\sigma(j)}))^{\lambda} \right)^{1/\lambda} \right) \end{array} \right) \end{array} \right)$$

where σ is a permutation of $\{1, 2, \ldots, n\}$ satisfying $S(\tilde{\alpha}_{\sigma(1)}) \geqslant S(\tilde{\alpha}_{\sigma(2)}) \geqslant \cdots \geqslant S(\tilde{\alpha}_{\sigma(n)})$, and $S(\cdot)$ is the reliability-aware score function defined in Definition 3.2. That is, the input RT-SFNs are first arranged in descending order according to the reliability-aware score function, and the ordered RT-SFNs are subsequently aggregated using the AA-ST multiplication operation under the ordered weight vector.

6. MAGDM Methodology based on RT-SFAAST Aggregation Operators

This section presents a reliability-aware MAGDM framework utilizing the proposed RT-SFAAST operators. Let $A = \{A_i\}_{i=1}^{m}$ be the set of alternatives, $C = \{C_j\}_{j=1}^{n}$ the evaluation criteria, and $E = \{E_k\}_{k=1}^{K}$ the expert panel. The expert weight vector $V = (v_1, \ldots, v_K)^T$ and criterion weight vector $W = (w_1, \ldots, w_n)^T$ are assumed to be predetermined. The MAGDM procedure consists of three systematic phases, as illustrated in Fig. 2 and summarized in Algorithm 1.

6.1. Phase I: Data Acquisition and Preprocessing

Step 1: Expert Information Elicitation. Each expert E_k assesses alternative A_i under criterion C_j using a linguistic pair (ℓ, r), where ℓ and r are performance and reliability terms selected from Table 1 and Table 2, respectively. These linguistic terms are subsequently mapped to an RT-SFN:

$$\tilde{\alpha}_{ij}^{(k)} = \left((\zeta_{ij}^{(k)}, \omega_{ij}^{(k)}, \upsilon_{ij}^{(k)}), (\delta_{ij}^{(k)}, \eta_{ij}^{(k)}, \beta_{ij}^{(k)}) \right)$$

This representation concurrently captures the membership information (MI), abstinence information (AbI), and non-membership information (NMI) alongside their corresponding reliability degrees (RDs) within a unified framework.

Step 2: Normalization for Criterion Type. To ensure mathematical comparability, cost-type criteria (C_c) are transformed into benefit-type (C_b) attributes. The normalized RT-SFN $\tilde{R}_{ij}^{(k)}$ is obtained by swapping the MI and NMI, alongside their respective RDs, to maintain semantic consistency:

$$\tilde{R}_{ij}^{(k)} = \begin{cases} \left((\zeta_{ij}^{(k)}, \omega_{ij}^{(k)}, \upsilon_{ij}^{(k)}), (\delta_{ij}^{(k)}, \eta_{ij}^{(k)}, \beta_{ij}^{(k)})\right), & \text{if } C_j \in C_b, \\ \left((\upsilon_{ij}^{(k)}, \omega_{ij}^{(k)}, \zeta_{ij}^{(k)}), (\beta_{ij}^{(k)}, \eta_{ij}^{(k)}, \delta_{ij}^{(k)})\right), & \text{if } C_j \in C_c. \end{cases} \tag{6.1}$$

6.2. Phase II: Reliability-Aware Information Fusion

Step 3: Group Consensus Construction. The individual expert decision matrices are fused into a collective matrix $\tilde{R} = [r_{ij}]_{m\times n}$. Using the proposed RT-SFAASTWA operator (Definition 5.1):

$$r_{ij} = \text{RT-SFAASTWA}(\tilde{R}_{ij}^{(1)}, \tilde{R}_{ij}^{(2)}, \ldots, \tilde{R}_{ij}^{(K)}; V) \tag{6.2}$$

This operator executes three sub-stages: mapping fuzzy evaluations into the periodic sine-trigonometric domain, performing weighted Aczél–Alsina aggregation, and recovering the collective components via domain inversion.

Step 4: Global Alternative Evaluation. The collective assessments r_{ij} are aggregated across criteria to determine each alternative's overall performance. The global assessment $\tilde{Q}_i$ for alternative A_i is computed using the criterion weight vector W:

$$\tilde{Q}_i = \text{RT-SFAASTWA}(r_{i1}, r_{i2}, \ldots, r_{in}; W) \tag{6.3}$$

6.3. Phase III: Prioritization and Robustness Analysis

Step 5: Score Computation and Final Ranking. The global assessments $\tilde{Q}_i$ are converted into crisp values using the reliability-aware score function $S(\tilde{Q}_i)$ (Eq. (3.3)). Alternatives are prioritized in descending order of their scores, with the accuracy function $A(\tilde{Q}_i)$ (Eq. (3.4)) used as a lexicographical tie-breaker.

Step 6: Sensitivity and Robustness Analysis. To evaluate the stability of the results, a sensitivity analysis is conducted by varying the Aczél–Alsina parameter λ and the rung parameter q. This step verifies the consistency of the decision-support outcomes across diverse risk attitudes.

Algorithm 1 MAGDM Procedure via RT-SFAAST Operators

Require: RT-SFN decision matrices $\tilde{R}^{(k)}$, weight vectors V and W.
Ensure: Prioritized ranking of alternatives A_i.

1: For each expert E_k and alternative A_i, normalize $\tilde{R}^{(k)}$ by swapping (ζ, δ) and (υ, β) for cost-type criteria.
2: Construct a collective matrix $[r_{ij}]$ by aggregating expert opinions using an RT-SFAAST operator.
3: Determine global assessments $\tilde{Q}_i$ using the criterion weight vector W.
4: Compute reliability-aware scores $S(\tilde{Q}_i)$ and accuracy values $A(\tilde{Q}_i)$.
5: Rank alternatives A_i in descending order of $S(\tilde{Q}_i)$ (using $A(\tilde{Q}_i)$ as a tie-breaker).

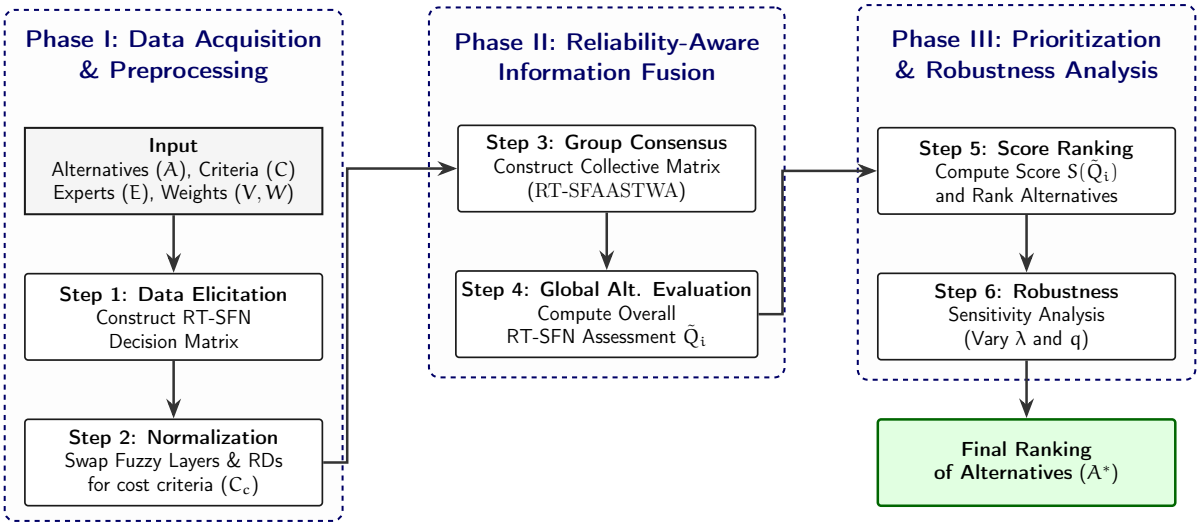


Figure 2: Framework of the proposed RT-SFAAST-based MAGDM methodology illustrating the three-phase decision-making process from data acquisition to final ranking.

7. Case Study: Smart Waste Management Interventions in Delhi

This section outlines the evaluation criteria and technical profiles of the five SWM interventions in Delhi. These descriptions and associated visual frameworks provide the evidentiary basis for the expert panel's linguistic assessments (Tables A.16–A.19) across all criteria.

7.1. Evaluation Criteria

The alternatives are evaluated against seven criteria (C_1–C_7) spanning technical, economic, operational, environmental, and social dimensions. These metrics were identified in the SWM literature and municipal planning frameworks [7, 28, 29, 30, 31]. Consistent with Section 6, criterion weights are assumed to be predetermined (Table 3) to focus on the application of the proposed RT-SFAAST operators.

Table 3: Evaluation criteria, attribute types, and weights for SWM prioritization

ID	Criterion	Type	Weight (w_j)
C_1	Effectiveness	Benefit	0.18
C_2	Cost	Cost	0.15
C_3	Efficiency	Benefit	0.14
C_4	Sustainability	Benefit	0.18
C_5	Scalability	Benefit	0.12
C_6	Acceptance	Benefit	0.13
C_7	Maintenance	Cost	0.10

7.2. Alternative A_1: IoT-Enabled Smart Bin Deployment

Alternative A_1 involves the citywide deployment of 1100 L semi-underground smart bins equipped with HC-SR04 ultrasonic sensors and a LoRa/GSM hybrid communication network [32, 28]. As illustrated in the integrated technical datasheet (Fig. 3), the system employs a dual-compartment design to facilitate source segregation, governed by a color-coded sensing logic in which fill levels exceeding 75% trigger automated, demand-driven collection requests [29]. Engineering data from Delhi-NCR pilots indicates that this intervention achieves a 20–40% reduction in bin overflows and a 30–40% decrease in transport-related emissions by eliminating unnecessary collection trips [32, 29]. However, the strategy requires significant capital expenditure and a projected cumulative land footprint of 500 acres for citywide retrofitting [33]. Operational reliability is highly sensitive to Delhi's environmental stressors; specifically, summer temperatures reaching 48°C and high airborne dust concentrations necessitate frequent sensor recalibration and battery replacements [34, 35]. These technical and infrastructural factors provided the evidentiary rationale for the RDs assigned to cost (C_2) and maintenance (C_7).



Figure 3: Technical datasheet (A_1): Sensing logic, Delhi-NCR operational photographs [29], and reliability stressors (heat/dust) utilized in the evaluation.

7.3. Alternative A_2: IoT-Based Waste Monitoring System

Alternative A_2 implements a metropolitan-scale digital traceability framework to manage Delhi's municipal waste [36]. As illustrated in the technical architecture (Fig. 4), the system centers on a Rs. 65 Crore Integrated Command and Control Centre (ICCC), which serves as a centralized monitoring hub [37]. The technical stack utilizes GPS-enabled collection vehicles, RFID-based traceability, and IoT-linked weighbridges to maintain a digital chain of custody from collection to final disposal sites [28, 36]. While the platform provides a digital audit trail supported by integrated CCTV feeds and automated sensor-to-MIS synchronization [36, 37], its reliability is affected by signal lag and packet loss in high-density corridors such as Old Delhi [34, 35]. These technical uncertainties regarding real-time connectivity and GPS drift provided the evidentiary basis used by experts to moderate the RDs of effectiveness (C_1), efficiency (C_3), and scalability (C_5).

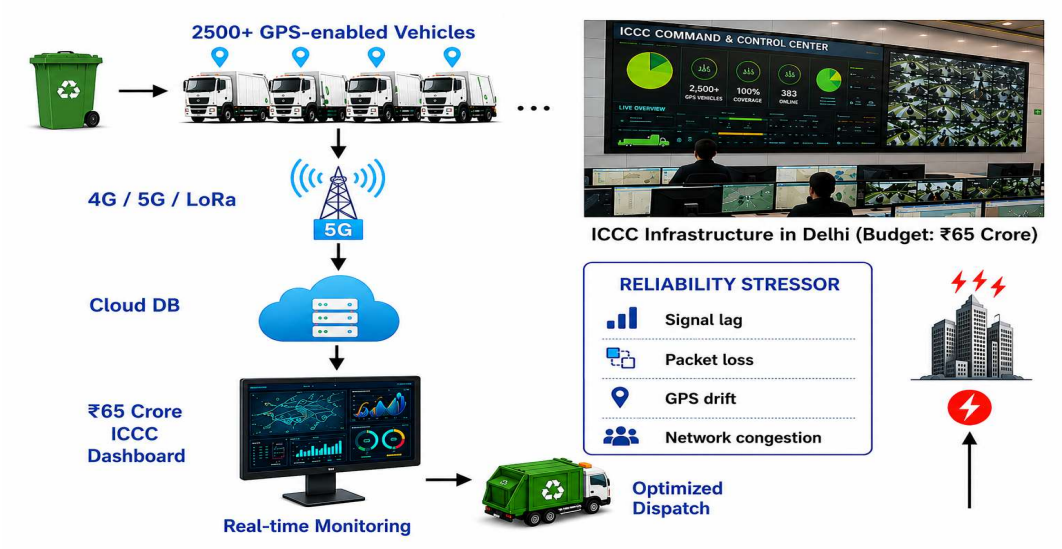


Figure 4: Technical architecture (A_2): Citywide data-fusion logic, Delhi ICCC photographs [37], and monitoring reliability stressors (signal lag) utilized in the evaluation.

7.4. Alternative A_3: AI-based Route Optimization

Alternative A_3 introduces an AI-driven decision layer utilizing Delhi's Rs. 100 crore Advanced Traffic System (ATS) for metropolitan-scale route optimization [38]. As illustrated in the intelligent path-planning

workflow (Fig. 5), the framework employs the Google Maps Distance Matrix API and a greedy nearest-neighbor (GNN) heuristic to compute optimal collection sequences for bins exceeding a 70% fill threshold [39]. The technical stack utilizes Long Short-Term Memory (LSTM) networks for predictive fill forecasting and MQTT protocols for 60-second data synchronization [39]. Engineering simulations demonstrate a reduction in average collection distance from 15 km to 10 km, a documented 33% improvement in operational efficiency [29, 39]. The operational stressors highlighted in the framework—specifically data latency from the ATS infrastructure, GPS drift in dense urban corridors, and driver resistance to algorithmic monitoring—provided the evidentiary rationale for the RDs assigned to efficiency (C_3) and public acceptance (C_6).

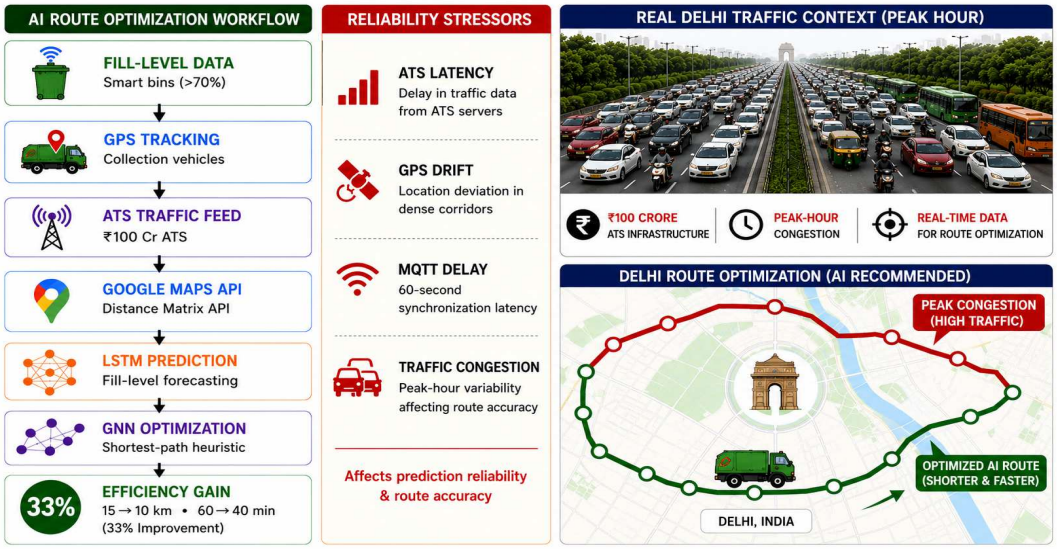


Figure 5: Technical framework (A_3): Path planning workflow, traffic heatmaps [38], and operational reliability stressors (data latency) utilized in the evaluation.

7.5. Alternative A_4: Automated Waste-Sorting Facilities

Alternative A_4 involves upgrading Delhi's 155 Material Recovery Facilities (MRFs) to automated centres, modeled after the Geeta Colony pilot in the Shahdara South Zone [33, 36]. The technical workflow depicted in Fig. 6 utilizes Near-Infrared (NIR) spectroscopy to identify material compositions, including plastics, paper, and metals, in milliseconds [40]. This high-speed identification enables robotic segregation arms to perform high-purity sorting, followed by vertical hydraulic baling, yielding 150 kg compressed bales for industrial recycling [41, 40]. While this intervention significantly increases throughput, industrial photography highlights critical reliability stressors: high airborne dust concentrations coat NIR lenses, and extreme summer temperatures attenuate the classification signal [41]. Furthermore, the informal circular economy introduces significant data uncertainty, as prior picking and sorting by waste collectors lead to inconsistent waste quality entering the automated stream [42, 40]. These technical and social complexities provided the evidentiary basis for the RDs assigned to sustainability (C_4), social acceptance (C_6), and maintenance (C_7).



Figure 6: Technical framework (A_4): Automated recovery workflow, Delhi industrial baseline photographs [40], and technical reliability stressors (dust) utilized in the evaluation.

7.6. Alternative A_5: Waste-to-Energy Capacity Expansion

Alternative A_5 involves the large-scale expansion of Delhi's Waste-to-Energy (WTE) infrastructure to address a municipal processing shortfall of 6,000 tonnes per day (TPD) [30]. Under a Rs. 1,753.77 crore roadmap, this strategy aims for a citywide processing capacity of 13,550 TPD through high-temperature incineration (850–1100°C), utilizing facilities such as the Tehkhand plant to generate between 20–60 MW of power [43, 31]. As illustrated in the thermal recovery workflow (Fig. 7), the process recovers energy from non-recyclable streams; however, the industrial baseline photographs highlight critical reliability stressors that moderate the alternative's efficiency. Specifically, the high moisture content of Delhi's mixed waste results in a calorific value of only 1,324 kcal/kg, significantly below the 1,800 kcal/kg threshold required for self-sustaining combustion and necessitating supplemental fuels [44, 45]. Furthermore, the proximity of plants to residential zones, located within a 100 m buffer (Fig. 7), has triggered health protests and frequent litigation, providing the evidentiary basis that experts use to moderate the RDs for efficiency (C_3), sustainability (C_4), and public acceptance (C_6).

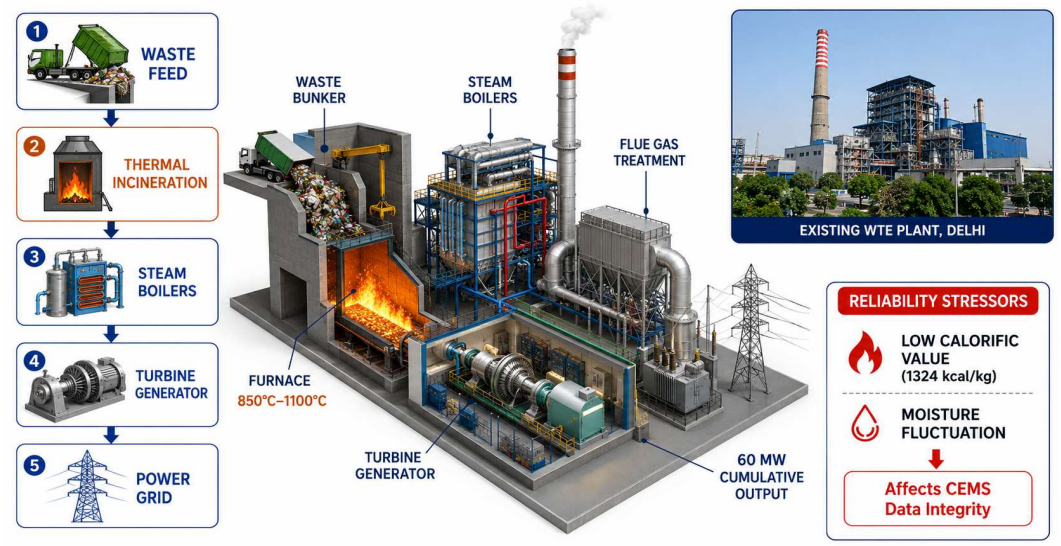


Figure 7: Technical framework (A_5): Thermal recovery workflow, Delhi industrial baseline photographs [44], and reliability stressors (moisture/proximity) utilized in the evaluation.

8. Results and Discussion

This section applies the MAGDM methodology of Section 6 to prioritize the smart waste management interventions described in Section 7, followed by sensitivity, comparative, and ablation analyses with practical implications.

8.1. Application of the Proposed MAGDM Methodology

The proposed MAGDM framework is applied using a panel of four domain experts, E_k $(k = 1, 2, 3, 4)$: an environmental engineer (E_1), a financial consultant (E_2), a smart city specialist (E_3), and an urban planner (E_4), with equal expert weight vector $V = (0.25, 0.25, 0.25, 0.25)^\mathsf{T}$. Each expert independently assesses alternative A_i under criterion C_j using a linguistic pair (ℓ, r) selected from Tables 1 and 2, forming the linguistic decision matrices in Section Appendix A, Tables A.16–A.19. Following Subsection 3.4, the rung parameter $q = 3$ and Aczél–Alsina parameter $\lambda = 2$ are adopted throughout.

8.2. Aggregation of Reliability T-Spherical Fuzzy Numbers

The linguistic decision matrices provided by the expert panel (Section Appendix A, Tables A.16–A.19) are aggregated using the proposed RT-SFAASTWA operator (Definition 5.1), following the two-stage procedure of Step 3 and Step 4 (Section 6). Both stages are traced explicitly for Alternative A_1 to illustrate the complete aggregation mechanism.

Stage I: Expert-Level Aggregation for $(\mathsf{A}_1, \mathsf{C}_1)$.. **Step 1 (Elicitation).** The linguistic assessments of A_1 under C_1 (Effectiveness) across the four experts are $\mathsf{E}_1 : (\mathrm{VG}, \mathrm{HR})$, $\mathsf{E}_2 : (\mathrm{G}, \mathrm{HR})$, $\mathsf{E}_3 : (\mathrm{VG}, \mathrm{HR})$, and $\mathsf{E}_4 : (\mathrm{G}, \mathrm{MR})$. Using Tables 1 and 2, these map to the RT-SFNs

$$\tilde{\alpha}_{11}^{(1)} = ((0.85, 0.10, 0.15), (0.85, 0.15, 0.15)), \qquad \tilde{\alpha}_{11}^{(2)} = ((0.75, 0.20, 0.25), (0.85, 0.15, 0.15)),$$
$$\tilde{\alpha}_{11}^{(3)} = ((0.85, 0.10, 0.15), (0.85, 0.15, 0.15)), \qquad \tilde{\alpha}_{11}^{(4)} = ((0.75, 0.20, 0.25), (0.70, 0.30, 0.30)).$$

Step 2 (Normalization). Since C_1 is benefit-type, $\tilde{\mathsf{R}}_{11}^{(k)} = \tilde{\alpha}_{11}^{(k)}$ for all k.

Step 3 (ST Transformation). Applying Eq. (4.1) with $q = 3$ gives $\mathcal{Z} \approx 0.919374$ for $\mathsf{E}_1, \mathsf{E}_3$ $(\zeta = 0.85)$ and $\mathcal{Z} \approx 0.788581$ for $\mathsf{E}_2, \mathsf{E}_4$ $(\zeta = 0.75)$; the corresponding $\mathcal{W}, \mathcal{V}$ values are negligible, on the order of 10^{-6}–10^{-4}.

Step 4 (Aczél–Alsina Weighted Summation). With $\lambda = 2$ and $\nu_k = 0.25$, the weighted logarithmic sum for the membership component is

$$\sum_{k=1}^{4} \nu_k(-\ln(1 - \mathcal{Z}_k))^2 \approx 0.5(-\ln(1 - 0.919374))^2 + 0.5(-\ln(1 - 0.788581))^2 \approx 4.377330.$$

Step 5 (Domain Inversion). Inverting the aggregated transformed values yields the collective RT-SFN for $(\mathsf{A}_1, \mathsf{C}_1)$:

$$\mathsf{r}_{11} = ((0.812728, 0.137488, 0.190205), (0.826186, 0.173814, 0.173814)).$$

The membership reliability degree $(\delta \approx 0.826)$ reflects strong group consensus, as three of the four experts independently reported High Reliability (HR).

Stage II: Criterion-Level Aggregation for A_1.. The same RT-SFAASTWA mechanism is subsequently applied across the seven collective RT-SFNs r_{1j} $(j = 1, \ldots, 7)$ obtained for A_1 (Section Appendix B), using the criterion weight vector $W = (0.18, 0.15, 0.14, 0.18, 0.12, 0.13, 0.10)^\mathsf{T}$ (Table 3). This produces the global assessment

$$\tilde{\mathsf{Q}}_1 = ((0.794589, 0.178255, 0.226578), (0.740024, 0.246327, 0.259976)).$$

Substituting into the score function (Eq. (3.3)) confirms

$$\mathsf{S}(\tilde{\mathsf{Q}}_1) = \frac{1 + (0.740024)(0.794589)^3 - (0.246327)(0.178255)^3 - (0.259976)(0.226578)^3}{2} \approx 0.6834,$$

consistent with the value reported for A_1 in Table 4. This confirms that the identical aggregation mechanism operates consistently at both the expert level (Stage I) and the criterion level (Stage II), providing a fully traceable path from linguistic elicitation to the final crisp score.

8.3. Overall Aggregation and Ranking Results

Applying Stage II of the aggregation procedure to all five alternatives yields the global assessments $\tilde{Q}_i$, which are converted into crisp score $S(\tilde{Q}_i)$ and accuracy $A(\tilde{Q}_i)$ values for prioritization (Table 4). All aggregated RT-SFNs satisfy the admissibility condition of Definition 3.1, numerically verifying the closure of the framework within the T-spherical fuzzy space. Alternatives are prioritized in descending order of $S(\tilde{Q}_i)$, utilizing $A(\tilde{Q}_i)$ as a lexicographical tie-breaker per Definition 3.3.

Table 4: Overall aggregated RT-SFNs, score values, accuracy values, and final ranking of the five SWM alternatives.

Alt.	**Global Assessment** $\tilde{Q}_i = ((\zeta, \omega, \upsilon), (\delta, \eta, \beta))$	$S(\tilde{Q}_i)$	$A(\tilde{Q}_i)$	**Rank**
A_1	$((0.7946, 0.1783, 0.2266), (0.7400, 0.2463, 0.2600))$	0.6834	0.3757	4
A_2	$((0.8656, 0.1141, 0.1453), (0.6985, 0.0011, 0.3015))$	0.7260	0.4539	2
A_3	$((0.8478, 0.1129, 0.1688), (0.7393, 0.2185, 0.2607))$	0.7245	0.4522	3
A_4	$((0.7936, 0.2047, 0.2272), (0.6781, 0.0000, 0.3219))$	0.6675	0.3426	5
A_5	$((0.8650, 0.1750, 0.1519), (0.9994, 0.0000, 0.0006))$	**0.8234**	**0.6467**	**1**

The resulting prioritization order is $A_5 \succ A_2 \succ A_3 \succ A_1 \succ A_4$, as illustrated in Fig. 8.

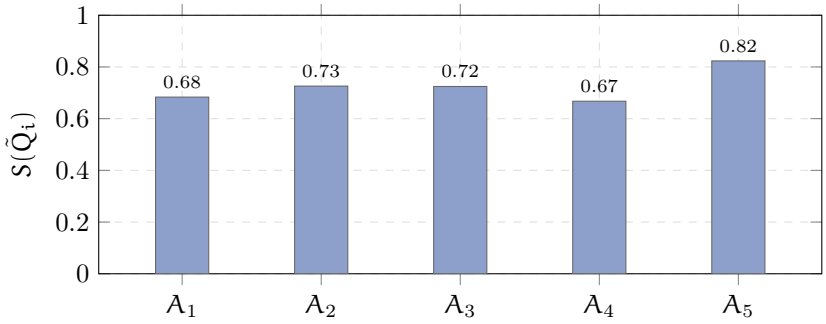


Figure 8: Score values $S(\tilde{Q}_i)$ and resulting prioritization of the five SWM interventions.

Waste-to-Energy Capacity Expansion (A_5) attains the highest score by a clear margin ($\Delta S \approx 0.10$ over the second-ranked alternative), driven primarily by its near-maximal reliability degree ($\delta \approx 0.999$), reflecting strong and consistent expert confidence despite the documented moisture and proximity stressors. IoT-Based Waste Monitoring (A_2) and AI-based Route Optimization (A_3) form a closely contested second tier, differing by only $\Delta S \approx 0.0015$; the accuracy function confirms $A_2 \succ A_3$, though this narrow margin warrants further scrutiny in the sensitivity analysis. IoT-Enabled Smart Bin Deployment (A_1) and Automated Waste-Sorting Facilities (A_4) occupy the lowest tier, consistent with the lower and more diffuse reliability degrees identified for their maintenance and sustainability criteria.

8.4. Interpretation of Ranking Results

The prioritization order aligns closely with the technical and reliability profiles established in Section 7. Alternative A_5 (Waste-to-Energy) ranks first primarily due to its high reliability across critical dimensions. Despite the moisture-content and plant-proximity stressors documented for efficiency (C_3) and acceptance (C_6), the expert panel maintained strong and consistent confidence in its effectiveness (C_1), which carries the highest criterion weight (0.18, Table 3). This highlights a key strength of the proposed RT-SFAASTWA operator: it does not automatically disqualify an alternative based on isolated reliability concerns; instead, it aggregates reliability information proportionally across all criteria. Consequently, an intervention with well-documented risks can still be prioritized if its overall expert confidence remains high across most attributes.

In contrast, A_1 and A_4 rank lowest, reflecting more diffuse, criterion-specific degradation in reliability. For A_1, this is driven by moderate confidence in cost (C_2) and maintenance (C_7). For A_4 (Automated Sorting), the degradation is more severe across sustainability (C_4), acceptance (C_6), and maintenance (C_7), with the cost assessment (C_2) acting as a significant bottleneck due to near-zero reliability ($\delta \approx 0.00$; Table B.20). These low-reliability assessments compound through criterion-level aggregation, yielding the

lowest overall membership reliability degrees among the five alternatives for A_1 and A_4 ($\delta \approx 0.74$ and $\delta \approx 0.68$, respectively; Table 4), compared with the near-maximal reliability of A_5.

The narrow margin between A_2 (IoT-Based Waste Monitoring) and A_3 (AI-Based Route Optimization), with scores differing by only $\Delta S \approx 0.0015$, suggests these interventions are approximately comparable in reliability-weighted performance. While A_2 is slightly superior in the baseline case, their proximity suggests that the ranking may be sensitive to the decision-maker's risk attitude or the choice of rung parameter. This localized instability is systematically examined in the following sensitivity analysis.

8.5. Reliability Impact Analysis

To evaluate the contribution of the proposed reliability layer, the RT-SFS results are compared against a reliability-free baseline obtained by setting all reliability degrees to unity ($\delta = \eta = \beta = 1$). According to Theorem 3.1(iii), this configuration reduces the framework to the classical T-SFS model, treating all assessments as absolute. Evaluation triplets $(\zeta, \omega, \upsilon)$ are kept unchanged to isolate the effect of the reliability degrees. Table 5 summarizes the resulting scores and rank variations.

Table 5: Comparison of RT-SFS scores against the reliability-free (T-SFS) baseline.

Alternative	$S_{\text{RT-SFS}}$	**Rank**	$S_{\text{T-SFS}}$	**Rank**	ΔS
A_1	0.6834	4	0.7422	4	-0.0588
A_2	0.7260	2	0.8220	1	-0.0960
A_3	0.7245	3	0.8016	3	-0.0771
A_4	0.6675	5	0.7397	5	-0.0722
A_5	0.8234	1	0.8191	2	$+0.0042$

The reliability-free baseline model yields the ranking $A_2 \succ A_5 \succ A_3 \succ A_1 \succ A_4$. The rank swap between A_5 and A_2 in the RT-SFS model demonstrates that reliability information is decision-critical; its omission leads to a materially different prioritization outcome.

The ΔS column quantifies the reliability penalty induced by incorporating expert confidence. Under RT-SFS, every alternative except A_5 suffers a significant score reduction, reflecting the RT-SFAASTWA operator's penalization of limited expert reliability. Waste-to-Energy Capacity Expansion (A_5) is minimally affected ($\Delta S \approx +0.004$) due to its near-maximal aggregated reliability degree ($\delta \approx 0.999$, Table 4). Conversely, IoT-Based Waste Monitoring (A_2) suffers the largest penalty (-0.0960) because its comparatively lower aggregated membership reliability degree ($\delta \approx 0.698$) is no longer masked by the unity assumption.

Practically, a reliability-unaware analysis would have prioritized IoT-Based Waste Monitoring (A_2). By explicitly accounting for expert confidence, RT-SFS instead identifies Waste-to-Energy Capacity Expansion (A_5) as the more robust optimal strategy, thereby preventing uncertainty masking during the decision-making process.

8.6. Sensitivity Analysis on Parameters and Weights

To evaluate the robustness of the prioritization results, a systematic sensitivity analysis is conducted across five dimensions: the Aczél–Alsina parameter (λ), the rung parameter (q), their joint variation, the criterion weight vector (W), and the expert weight vector (V). Ranking stability is quantified using Spearman's rank correlation coefficient (ρ_s), which compares the baseline ranking (Table 4) with each perturbed ranking:

$$\rho_s = 1 - \frac{6 \sum_{i=1}^{m} d_i^2}{m(m^2 - 1)}, \tag{8.1}$$

where d_i denotes the difference in rank positions for alternative A_i, and $m = 5$. A ρ_s value close to 1 indicates strong ranking stability and, consequently, methodological robustness. The results, summarized in Fig. 9, demonstrate high methodological stability.

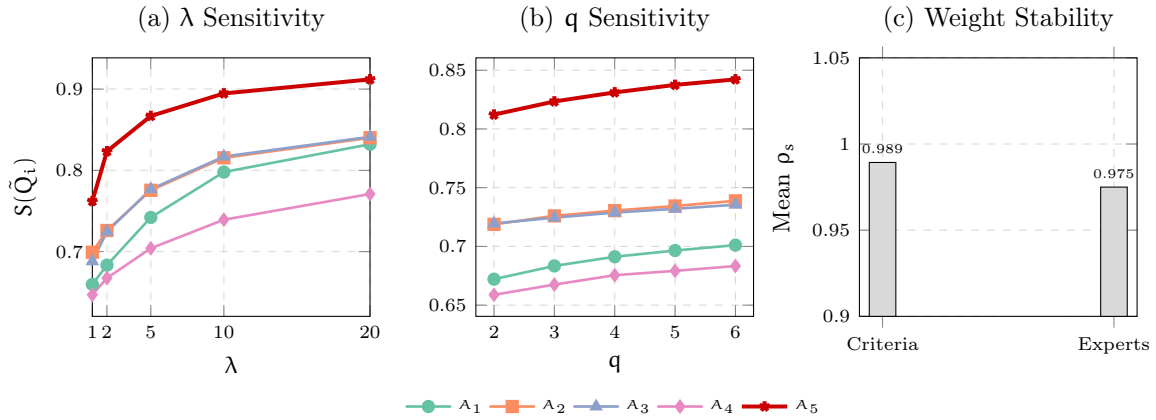


Figure 9: Summary of the sensitivity analysis: (a) score variations with the Aczél–Alsina parameter λ; (b) score variations with the rung parameter q; and (c) mean Spearman rank correlation coefficients under criterion and expert weight perturbations.

8.6.1. Effect of the Aczél–Alsina Parameter λ

The rung parameter is fixed at $q = 3$, and the global assessments are recomputed for $\lambda \in \{1, 1.5, 2, 3, 4, 5, 7, 10, 15, 20\}$. Table 6 summarizes the resulting score values and ranking stability.

Table 6: Alternative scores and ranking stability under variation of the AA parameter λ.

Alt.	λ=1	λ=1.5	λ=2	λ=3	λ=4	λ=5	λ=7	λ=10	λ=15	λ=20
A_1	0.6597	0.6719	0.6834	0.7049	0.7245	0.7421	0.7705	0.7979	0.8208	0.8321
A_2	0.6993	0.7140	0.7260	0.7458	0.7620	0.7755	0.7961	0.8154	0.8318	0.8401
A_3	0.6882	0.7094	0.7245	0.7464	0.7631	0.7768	0.7977	0.8170	0.8332	0.8412
A_4	0.6469	0.6586	0.6675	0.6820	0.6939	0.7041	0.7209	0.7393	0.7590	0.7709
A_5	0.7621	0.8060	0.8234	0.8433	0.8567	0.8669	0.8814	0.8946	0.9061	0.9119
ρ_s	1.000	1.000	1.000	0.900	0.900	0.900	0.900	0.900	0.900	0.900

The scores of all alternatives increase monotonically as λ increases, reflecting the progressively stricter aggregation behavior of the Aczél–Alsina operators. Alternative A_5 consistently remains the top priority, and A_4 remains the lowest-ranked across the entire parameter range. A single rank reversal occurs at $\lambda \geqslant 3$, where A_2 and A_3 swap positions ($\rho_s = 0.900$). This localized instability is expected given the marginal baseline score difference between these two alternatives ($\Delta S \approx 0.0015$). Nevertheless, the invariance of the top-ranked alternative (A_5) demonstrates that the overall decision outcome is robust to variations in the decision-maker's risk attitude.

8.6.2. Effect of the Rung Parameter and Joint Sensitivity Analysis

The influence of the rung parameter on the non-linear aggregation behavior was first evaluated by varying $q \in \{2, 3, 4, 5, 6\}$ while holding $\lambda = 2$ fixed. As shown in Table 7, the prioritization results are invariant to q across most of the tested range ($q \geqslant 3$). An isolated rank reversal between A_2 and A_3 occurs at $q = 2$, corresponding to the conventional spherical fuzzy set (SFS) special case. To ensure that no interaction between risk attitude (λ) and uncertainty granularity (q) would alter the primary decision, a joint sensitivity analysis was performed. A 5×4 parameter grid spanning $\lambda \in \{1, 2, 5, 10, 20\}$ and $q \in \{2, 3, 4, 5\}$ was evaluated, with the top-ranked alternative identified for each of the 20 parameter configurations (Table 8).

Table 7: Ranking and Spearman stability under q variation ($\lambda = 2$ fixed).

q	**Ranking**	ρ_s
2	$A_5 \succ A_3 \succ A_2 \succ A_1 \succ A_4$	0.900
3	$A_5 \succ A_2 \succ A_3 \succ A_1 \succ A_4$	1.000
4	$A_5 \succ A_2 \succ A_3 \succ A_1 \succ A_4$	1.000
5	$A_5 \succ A_2 \succ A_3 \succ A_1 \succ A_4$	1.000
6	$A_5 \succ A_2 \succ A_3 \succ A_1 \succ A_4$	1.000

Table 8: Top-ranked alternative across the joint (λ, q) parameter grid.

$\lambda \backslash q$	$q = 2$	$q = 3$	$q = 4$	$q = 5$
1	A_5	A_5	A_5	A_5
2	A_5	A_5	A_5	A_5
5	A_5	A_5	A_5	A_5
10	A_5	A_5	A_5	A_5
20	A_5	A_5	A_5	A_5

The results demonstrate complete consistency of the optimal decision: Waste-to-Energy Capacity Expansion (A_5) remains the highest-priority intervention across all individual q variations and all 20 joint parameter configurations. This stability confirms that the proposed RT-SFAAST framework is robust to the simultaneous variation of both the Aczél–Alsina parameter and the rung parameter, indicating that the optimal decision is independent of the specific combination of risk attitude and uncertainty granularity selected by the decision-maker.

8.6.3. Sensitivity to Criterion and Expert Weights

To evaluate the robustness of the proposed MAGDM framework with respect to weight assignment, a systematic perturbation analysis was conducted for both the criterion weight vector (W) and the expert weight vector (V). First, each criterion weight w_j was individually perturbed by $\pm 10\%$ and $\pm 20\%$, while the remaining weights were proportionally renormalized, yielding 28 configurations. Second, the equal expert-weight assumption was relaxed by assigning each expert a dominant weight of 40%, 50%, and 60% in turn, yielding 12 additional configurations. Table 9 summarizes the ranking stability across all 40 configurations.

Table 9: Summary of ranking stability under criteria and expert weight perturbation.

Perturbation Source	**Configurations**	**Mean ρ_s**	**Min ρ_s**
Criteria weights W ($\pm 10\%, \pm 20\%$ per criterion)	28	0.9893	0.9000
Expert weights V (one expert dominant at 40–60%)	12	0.9750	0.9000

Of the 28 criteria weight perturbations, 25 leave the ranking entirely unchanged ($\rho_s = 1.000$). Only three specific cases (w_3 increased by 20%, w_4 decreased by 20%, or w_6 decreased by 20%) produce the isolated rank reversal between A_2 and A_3 ($\rho_s = 0.900$). Similarly, the expert weights remain stable in 9 of the 12 cases. The same A_2/A_3 reversal occurs consistently when Expert E_1 (the environmental engineer) is made dominant. This indicates that while E_1's environmental-engineering assessment of the two technically adjacent interventions (A_2 and A_3) slightly diverges from the panel average, the divergence is confined to a single middle-tier transposition.

Critically, across all 40 weight-related configurations, Waste-to-Energy Capacity Expansion (A_5) and Automated Waste-Sorting Facilities (A_4) consistently maintain their respective first and last positions. This overall stability demonstrates that the proposed MAGDM methodology is robust to significant variations in the relative importance assigned to both decision criteria and individual expert opinions.

8.6.4. Summary of Sensitivity Findings

The cumulative results of the 75 sensitivity configurations, spanning variations in λ, q, their joint interaction, and perturbations of the criterion and expert weight vectors (W and V), confirm the robustness of the proposed RT-SFAAST-based MAGDM framework. Across all tested scenarios, Waste-to-Energy Capacity Expansion (A_5) and Automated Waste-Sorting Facilities (A_4) consistently retain the first and last ranking positions, respectively. The only observed variation is a recurring adjacent rank reversal between IoT-Based Waste Monitoring (A_2) and AI-based Route Optimization (A_3), consistent with their marginal baseline score difference ($\Delta S \approx 0.0015$).

This localized variation demonstrates the discriminative capability of the proposed framework, which distinguishes genuinely competitive alternatives while preserving stable rankings for alternatives supported by stronger and more consistent expert evidence. Overall, the sensitivity analysis confirms that the

proposed methodology provides robust and reliable decision support for smart urban waste management planning.

8.7. Comparative Analysis

This section presents a multi-dimensional comparative evaluation of the proposed RT-SFAAST framework to establish its mathematical consistency, strategic flexibility, and comparative effectiveness. The analysis is structured into four investigative layers: (i) a rationale for the Aczél–Alsina selection via benchmarking against alternative Archimedean t-norm families; (ii) an internal family comparison between arithmetic and geometric operators to demonstrate policy-driven versatility; (iii) an ablation study to quantify the discriminative refinement provided by the sine-trigonometric transformation; and (iv) a benchmark against published T-spherical fuzzy operators. Fig. 10 provides a visual synthesis of these findings, highlighting the dispersion characteristics, strategic adaptability, discriminative refinement, and comparative performance of the proposed framework.

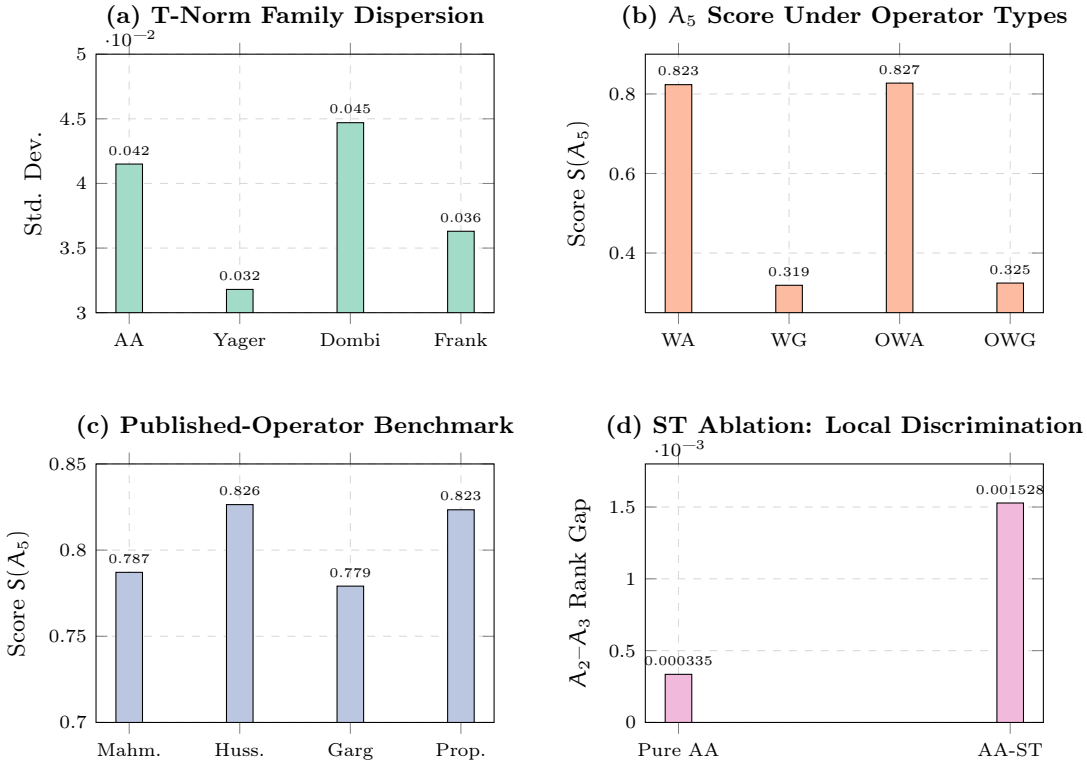


Figure 10: Comparative analysis dashboard: (a) score dispersion across the selected Archimedean t-norm families; (b) score variation of $\mathcal{A}_5$ across the proposed arithmetic and geometric operator types; (c) $\mathcal{A}_5$ priority scores under the proposed and published T-spherical fuzzy operators; and (d) improvement in the $\mathcal{A}_2$–$\mathcal{A}_3$ discrimination gap resulting from the sine-trigonometric transformation.

8.7.1. Rationale for the Aczél–Alsina t-Norm Family

To justify the selection of the Aczél–Alsina (AA) family [17], it is benchmarked against the Yager [46], Dombi [47], and Frank [48] Archimedean families. To isolate the influence of the t-norm selection, the reliability and sine-trigonometric layers are omitted ($\lambda = \mathfrak{p} = \mathfrak{s} = 2, \mathfrak{q} = 3$), reducing the model to a standard T-SFS baseline. Table 10 provides the additive generators for each family, while Table 11 summarizes the comparative benchmarking results.

Table 10: Additive generators and structural properties of the compared Archimedean families.

Family	**Generator** $g(t)$	**Inverse** $g^{-1}(y)$	**Structural Note**
AA [17]	$(-\ln t)^{\lambda}$	$\exp(-y^{1/\lambda})$	Permits a consistent boundary treatment in the proposed formulation.
Yager [46]	$(1-t)^{p}$	$1-\min(1, y^{1/p})$	Explicitly bounded mechanism; saturates once the weighted sum exceeds unity.
Dombi [47]	$((1-t)/t)^{p}$	$1/(1+y^{1/p})$	Ratio-based generator; requires specific limiting considerations at the boundary $t=0$.
Frank [48]	$-\ln((s^{t}-1)/(s-1))$	$\ln(1+(s-1)e^{-y})/\ln s$	Log-exponential form; requires separate treatment for the degenerate case $s=1$.

Table 11: Benchmarking of score values and rankings across t-norm families ($\lambda = p = s = 2$) on the reliability-free and ST-free baseline data.

Family	$S(A_1)$	$S(A_2)$	$S(A_3)$	$S(A_4)$	$S(A_5)$	**Std. Dev.**	**Top Rank**	**Overall Ranking**
AA [17]	0.7490	0.8274	0.8083	0.7436	0.8264	0.0415	A_2	$A_2 \succ A_5 \succ A_3 \succ A_1 \succ A_4$
Yager [46]	0.7044	0.7823	0.7410	0.7074	0.7244	0.0318	A_2	$A_2 \succ A_3 \succ A_5 \succ A_4 \succ A_1$
Dombi [47]	0.7965	0.8632	0.8472	0.7641	0.8641	0.0447	A_5	$A_5 \succ A_2 \succ A_3 \succ A_1 \succ A_4$
Frank [48]	0.7184	0.8017	0.7685	0.7244	0.7815	0.0363	A_2	$A_2 \succ A_5 \succ A_3 \succ A_4 \succ A_1$

Table 12: Parameter sensitivity sweep for each t-norm family conducted on the reliability-free and ST-free T-SFS baseline.

Family	**Param.**	**Overall Ranking**	**Std. Dev.**
AA [17]	$\lambda = 1$	$A_2 \succ A_5 \succ A_3 \succ A_4 \succ A_1$	0.0372
	$\lambda = 2$	$A_2 \succ A_5 \succ A_3 \succ A_1 \succ A_4$	0.0415
	$\lambda = 3$	$A_5 \succ A_2 \succ A_3 \succ A_1 \succ A_4$	0.0421
	$\lambda = 5$	$A_5 \succ A_2 \succ A_3 \succ A_1 \succ A_4$	0.0414
	$\lambda = 10$	$A_2 \succ A_5 \succ A_3 \succ A_1 \succ A_4$	0.0395
Yager [46]	$p = 1$	$A_2 \succ A_3 \succ A_4 \succ A_1 \succ A_5$	0.0346
	$p = 2$	$A_2 \succ A_3 \succ A_5 \succ A_4 \succ A_1$	0.0318
	$p = 3$	$A_2 \succ A_3 \succ A_5 \succ A_1 \succ A_4$	0.0321
	$p = 5$	$A_2 \succ A_3 \succ A_5 \succ A_1 \succ A_4$	0.0329
	$p = 10$	$A_2 \succ A_3 \succ A_5 \succ A_1 \succ A_4$	0.0345
Dombi [47]	$p = 1$	$A_2 \succ A_5 \succ A_3 \succ A_1 \succ A_4$	0.0425
	$p = 2$	$A_5 \succ A_2 \succ A_3 \succ A_1 \succ A_4$	0.0447
	$p = 3$	$A_2 \succ A_5 \succ A_3 \succ A_1 \succ A_4$	0.0444
	$p = 5$	$A_2 \succ A_5 \succ A_3 \succ A_1 \succ A_4$	0.0431
	$p = 10$	$A_2 \succ A_5 \succ A_3 \succ A_1 \succ A_4$	0.0376
Frank [48]	$s = 2$	$A_2 \succ A_5 \succ A_3 \succ A_4 \succ A_1$	0.0363
	$s = 3$	$A_2 \succ A_5 \succ A_3 \succ A_4 \succ A_1$	0.0358
	$s = 5$	$A_2 \succ A_5 \succ A_3 \succ A_4 \succ A_1$	0.0352
	$s = 10$	$A_2 \succ A_5 \succ A_3 \succ A_4 \succ A_1$	0.0344

The comparative analysis reveals that, while the Dombi family attains a marginally higher score dispersion (0.0447) than the AA family (0.0415), selecting a t-norm family entails trade-offs between score dispersion and mathematical structure. Yager exhibits strong sensitivity at $p = 1$ (Table 12), where the bounded aggregation mechanism substantially alters the resulting scores and moves A_5 to the last position. Furthermore, the Frank and Dombi families require specific analytical treatment at parameter or boundary limits, introducing additional complexity into the mathematical formulation.

The adoption of the AA family is based on three foundational considerations. First, its logarithmic generator provides a smooth, monotonic parameterized structure that integrates naturally with the

proposed framework while allowing appropriate limiting treatment at the boundaries. Second, the AA formulation provides the mathematical basis for the formal properties of the proposed RT-SFAASTWA operator, including boundedness, idempotency, and monotonicity, established in Theorems 5.1–5.4. Third, the single parameter λ enables systematic sensitivity analysis while preserving a consistent aggregation structure. Therefore, although alternatives such as Dombi may offer greater score dispersion in certain instances, the AA family provides the most suitable balance among mathematical tractability, analytical consistency, and parameterized flexibility for the proposed reliability-aware methodology.

8.7.2. Comparative Analysis of the RT-SFAAST Operator Family

Sections 8.3–8.6 utilize the RT-SFAASTWA operator to establish a baseline prioritization. To validate the functional flexibility of the proposed framework, this section applies the remaining family members—RT-SFAASTWG, RT-SFAASTOWA, and RT-SFAASTOWG—to the identical Delhi case study data ($\lambda = 2, q = 3$). Table 13 summarizes the scores, resulting rankings, and information discrimination power (quantified via the standard deviation of scores) across the four operators.

Table 13: Comprehensive comparison of scores, rankings, and discrimination power across the RT-SFAAST operator family.

	RT-SFAAST Operators			
Metric	**WA**	**WG**	**OWA**	**OWG**
$S(A_1)$	0.6834	0.5638	0.6852	0.5657
$S(A_2)$	0.7260	0.4455	0.7293	0.4437
$S(A_3)$	0.7245	0.4470	0.7312	0.4619
$S(A_4)$	0.6675	0.4490	0.6644	0.4477
$S(A_5)$	0.8234	0.3189	0.8273	0.3245
Ranking	$A_5 \succ A_2 \succ A_3 \succ A_1 \succ A_4$	$A_1 \succ A_4 \succ A_3 \succ A_2 \succ A_5$	$A_5 \succ A_3 \succ A_2 \succ A_1 \succ A_4$	$A_1 \succ A_3 \succ A_4 \succ A_2 \succ A_5$
Std. Dev.	0.0606	0.0867	0.0628	0.0856

The results reveal a striking divergence: the arithmetic-type operators (WA and OWA) prioritize Waste-to-Energy Capacity Expansion (A_5), whereas the geometric-type operators (WG and OWG) rank it last. This is not a mathematical inconsistency but a direct consequence of the non-compensatory character of geometric aggregation. Under WA/OWA, A_5's exceptional performance in effectiveness (C_1, $\delta = 1.000$) compensates for its low-scoring, low-reliability assessment in public acceptance (C_6), which reflects the health-protest and litigation risks documented in Section 7.6. Conversely, the geometric-type operators do not permit such trade-offs; A_5's poor performance in a single criterion acts as a "veto," depressing its overall score below every other alternative.

This divergence equips decision-makers with two complementary aggregation strategies within a unified reliability-aware framework. The WA/OWA operators are suitable for **compensatory assessments**, where overall utility is maximized. In contrast, the WG/OWG operators support a **precautionary policy**, where significant risk in even a single dimension (such as public acceptance) is sufficient to moderate the priority of an alternative. Furthermore, the geometric-type operators achieve approximately 40% higher discrimination power (Std. Dev. ≈ 0.086) than their arithmetic counterparts, effectively sharpening the distinctions between closely contested alternatives. These findings demonstrate that the proposed RT-SFAAST framework is mathematically robust and sufficiently versatile to support both compensatory and non-compensatory decision strategies within a unified reliability-aware decision-making framework.

8.7.3. Ablation Study: Effect of the Sine-Trigonometric Transformation

The introduction of the Sine-Trigonometric (ST) layer was motivated by its reported capability to enhance discrimination between closely related fuzzy evaluations [21]. To verify this benefit within the proposed RT-SFAAST framework, this section conducts an ablation study by comparing the proposed operator against a Pure Aczél–Alsina (Pure AA) variant. Following Remark 4.1(ii), the Pure AA variant replaces the ST transformation with the identity mapping while retaining the reliability layer. Table 14 summarizes the scores and discrimination metrics for both models on the identical Delhi case study data ($\lambda = 2, q = 3$).

Table 14: Ablation analysis comparing Pure Aczél–Alsina and the proposed AA-ST operators.

Variant	$S(A_1)$	$S(A_2)$	$S(A_3)$	$S(A_4)$	$S(A_5)$	**Rank Gap** (A_2, A_3)	**Std. Dev.**	**Ranking**
Pure AA	0.6884	0.7298	0.7294	0.6700	0.8304	0.000335	0.0621	$A_5 \succ A_2 \succ A_3 \succ A_1 \succ A_4$
AA-ST	0.6834	0.7260	0.7245	0.6675	0.8234	0.001528	0.0606	$A_5 \succ A_2 \succ A_3 \succ A_1 \succ A_4$

The results confirm that while both variants yield the same ranking, the ST transformation provides critical refinement of the decision basis. The overall score standard deviation remains largely consistent, as it is dominated by the already well-separated alternatives. However, the minimum adjacent-rank gap—the margin between the single closest-contested pair, A_2 and A_3—increases from 0.000335 to 0.001528.

This represents a 355.4% improvement in local discrimination. Under the Pure AA model, the separation between A_2 and A_3 is so narrow that the ranking is highly vulnerable to minor data perturbations. The ST transformation enlarges this margin nearly fivefold, providing a materially more stable basis for the prioritization. This finding refines the understanding of sine-trigonometric operators: their primary utility within the RT-SFAAST framework is not to uniformly inflate variance, but to stabilize decisions between closely competing alternatives where discrimination is mathematically hardest.

8.7.4. Comparison with Existing Published Operators

The comparisons in Sections 5.5 through 5.8 provide internal validation for the proposed framework. To situate the proposed RT-SFAASTWA operator against the wider literature, this section benchmarks it against three established T-spherical fuzzy weighted averaging operators: the original algebraic operator [13], the Aczél–Alsina operator [20], and the sine-trigonometric operator [23]. For a fair comparison, the benchmark operators are applied to the identical Delhi case study data ($q = 3$), while the proposed framework is evaluated with its reliability layer enabled. For reference, setting all reliability degrees to unity reduces the proposed score function to a reliability-free T-spherical fuzzy form (Theorem 3.1(iii)). Table 15 summarizes the comparative results.

Table 15: Benchmark analysis: Comparison between the proposed RT-SFAASTWA and existing T-SFS operators.

Method	$S(A_1)$	$S(A_2)$	$S(A_3)$	$S(A_4)$	$S(A_5)$	**Std.Dev.**	**Min.Gap**	**Overall Ranking**
Mahmood et al. [13]	0.7212	0.8046	0.7736	0.7262	0.7871	0.0372	0.0050	$A_2 \succ A_5 \succ A_3 \succ A_4 \succ A_1$
Hussain et al. [20]	0.7490	0.8274	0.8083	0.7436	0.8264	0.0415	0.0010	$A_2 \succ A_5 \succ A_3 \succ A_1 \succ A_4$
Garg et al. [23]	0.7174	0.8009	0.7660	0.7236	0.7791	0.0360	0.0063	$A_2 \succ A_5 \succ A_3 \succ A_4 \succ A_1$
Proposed	0.6834	0.7260	0.7245	0.6675	0.8234	0.0606	0.0015	$A_5 \succ A_2 \succ A_3 \succ A_1 \succ A_4$

The results show that all three benchmark operators prioritize IoT-Based Waste Monitoring System (A_2), whereas the proposed RT-SFAASTWA operator identifies Waste-to-Energy Expansion (A_5) as the top priority. This reversal is attributable to the reliability layer. Conventional methods, including the Aczél–Alsina operator of Hussain et al. [20], implicitly assume absolute expert confidence, thereby masking the lower reliability consensus ($\delta \approx 0.698$) associated with A_2 compared to the near-maximal reliability ($\delta \approx 0.999$) assigned to A_5. While Hussain et al. introduced the flexibility of the AA aggregation to T-spherical fuzzy sets, their model lacks the corrective mechanism provided by the reliability triplet. By explicitly accounting for these differing confidence levels, the proposed framework identifies A_5 as the genuine optimal intervention.

Furthermore, the proposed method exhibits the largest overall score dispersion, with a standard deviation of 0.0606, representing an increase of approximately 46% to 68% over the benchmark methods. While the methods by Mahmood et al. [13] and Garg et al. [23] report a larger minimum adjacent-rank gap, their margins lie between A_4 and A_1, which the proposed method separates comfortably. In contrast, the proposed method correctly localizes its narrowest margin between A_2 and A_3 ($\Delta S \approx 0.0015$). This identifies a genuinely close contest that is independently verified by the sensitivity analysis in Section 5.6, where A_2 and A_3 were the only alternatives to exhibit rank reversals under perturbation. Collectively, these findings demonstrate that the proposed RT-SFAASTWA framework provides more informative decision support by uncovering reliability-driven variations that conventional T-spherical fuzzy models fail to detect.

8.8. Limitations

Despite the demonstrated robustness of the proposed framework, several limitations remain.

(i) **Predetermined weights.** The criterion weight vector W (Table 3) and expert weight vector V were fixed *a priori* rather than derived using a formal weight-elicitation method. Nevertheless, the sensitivity analysis (Section 8.6) confirms the stability of the ranking under weight perturbations.

(ii) **Subjective reliability elicitation.** The reliability triplets (δ, η, β) were elicited from experts rather than derived from objective data-driven indicators, retaining an element of expert subjectivity.

(iii) **Single-context validation.** The case study considers one metropolitan context (Delhi), five alternatives, and a four-member expert panel; thus, generalizability to other contexts remains to be established.

(iv) **Fixed baseline parameters.** The Aczél–Alsina parameter λ and rung parameter q were specified as baseline values and evaluated through systematic sensitivity analysis (Section 8.6), rather than determined through a formal parameter-selection procedure.

(v) **Scalability.** The computational performance of the nested exponential, logarithmic, and inverse-trigonometric operations in the AA-ST operators (Definition 4.4) has not been benchmarked for substantially larger MAGDM instances.

These limitations define the scope of the present study and provide directions for future research, as outlined in Section 9.

9. Conclusion and Future Work

This paper proposed the RT-SFS as a reliability-aware extension of the T-spherical fuzzy framework and developed four AA-ST aggregation operators, namely RT-SFAASTWA, RT-SFAASTWG, RT-SFAASTOWA, and RT-SFAASTOWG. The proposed operators integrate reliability information with a parameterized Aczél–Alsina aggregation and a sine-trigonometric transformation, and their fundamental properties, including boundedness, idempotency, and monotonicity, were formally established.

The proposed reliability-aware MAGDM framework was applied to prioritize five smart waste management interventions in Delhi, India. The resulting ranking, $A_5 \succ A_2 \succ A_3 \succ A_1 \succ A_4$, identifies Waste-to-Energy Capacity Expansion as the top-priority intervention. Comparison with the reliability-free baseline demonstrates that incorporating reliability information can materially alter the final prioritization. The sensitivity analysis confirmed the stability of the primary recommendation under variations in model parameters, criteria, and expert weights, while the comparative and ablation analyses demonstrated the flexibility of the operator family and the enhanced discrimination provided by the sine-trigonometric transformation. These findings support the applicability of the proposed framework to reliability-sensitive MAGDM problems in sustainable urban infrastructure planning. Building on the identified limitations, future work may consider:

- **Objective weight determination** using BWM, AHP, or entropy-based methods to reduce subjectivity in weight assignment.
- **Data-driven reliability estimation** using historical, sensor, or expert-performance data.
- **Multi-city validation** across diverse urban, infrastructural, and socioeconomic contexts.
- **Adaptive parameter learning** for automatically selecting λ and q from decision data.
- **Dynamic and large-scale extensions** for time-evolving assessments and larger MAGDM problems.
- **Hybrid uncertainty frameworks** incorporating interval-valued or hesitant fuzzy extensions.

Declaration of Generative AI and AI-assisted Technologies

During the preparation of this manuscript, ChatGPT (OpenAI) and Google AI Studio were used solely for language editing and rewriting. The authors reviewed and edited the AI-assisted output and take full responsibility for the content of the manuscript.

Code Availability

The Scilab code used in this study is available from the corresponding author upon reasonable request.

Declaration of Competing Interest

The authors declare that they have no known competing financial or personal interests that could have influenced the work reported in this paper.

References

[1] E. Cook, K. Ionkova, P. Bhada-Tata, S. Yadav, What a Waste 3.0: Global Snapshot of Solid Waste Management toward Circularity until 2050, World Bank Group, Washington, DC, 2026, accessed on 17 June 2026. doi:10.1596/978-1-4648-2309-1.
URL https://doi.org/10.1596/978-1-4648-2309-1

[2] Statistics Times, Population of India, accessed on 17 June 2026 (2025).
URL https://statisticstimes.com/demographics/country/india-population.php

[3] Government of NCT of Delhi, Economic Survey of Delhi 2025–26, accessed on 10 August 2026 (2026).
URL https://delhiplanning.delhi.gov.in/sites/default/files/2026-03/economic_survey_english_0.pdf

[4] The Indian Express, Mumbai generated over 9,800 tonnes of solid waste daily as against BMC's claim: CAG report flags glaring discrepancies, accessed on 17 June 2026 (2025).
URL https://indianexpress.com/article/cities/mumbai/mumbai-solid-waste-bmc-cag-report-9909388/

[5] S. B. J. Singh, Hyderabad grapples with mounting municipal waste, the New Indian Express, accessed on 17 June 2026 (2025).
URL https://www.newindianexpress.com/cities/hyderabad/2025/Feb/10/hyderabad-grapples-with-mounting-municipal-waste

[6] BIN - Brands In Nature, Waste Management in Pune 2026: Key Data, Tech. rep., Pune Municipal Corporation, accessed on 17 June 2026 (2026).
URL https://joinbin.com/waste-management-pune

[7] Devika Kannan and Shakiba Khademolqorani and Nassibeh Janatyan and Somaieh Alavi, Smart waste management 4.0: The transition from a systematic review to an integrated framework, Waste Management 174 (2024) 1–18. doi:10.1016/j.wasman.2023.08.041.

[8] L. A. Zadeh, Fuzzy sets, Information and control 8 (3) (1965) 338–353. doi:10.1016/S0019-9958(65)90241-X.

[9] K. T. Atanassov, Intuitionistic fuzzy sets, Fuzzy sets and Systems 20 (1) (1986) 87–96. doi:10.1016/S0165-0114(86)80034-3.

[10] R. R. Yager, Pythagorean fuzzy subsets, in: 2013 Joint IFSA World Congress and NAFIPS Annual Meeting (IFSA/NAFIPS), IEEE, 2013, pp. 57–61. doi:10.1109/IFSA-NAFIPS.2013.6608375.

[11] R. R. Yager, Generalized Orthopair Fuzzy Sets, IEEE Transactions on Fuzzy Systems 25 (5) (2017) 1222–1230. doi:10.1109/TFUZZ.2016.2604005.

[12] B. C. Cuong, V. Kreinovich, Picture Fuzzy Sets – A New Concept for Computational Intelligence Problems, in: Proceedings of the 2013 Third World Congress on Information and Communication Technologies (WICT), 2013, pp. 1–6. doi:10.1109/WICT.2013.7113099.

[13] T. Mahmood, K. Ullah, Q. Khan, N. Jan, An Approach Towards Decision Making and Medical Diagnosis Problems Using the Concept of Spherical Fuzzy Sets, Neural Computing and Applications 31 (11) (2019) 7041–7053. doi:10.1007/s00521-018-3521-2.

[14] M. Riaz, M. R. Hashmi, Linear Diophantine Fuzzy Set and Its Applications Towards Multi-Attribute Decision-Making Problems, Journal of Intelligent & Fuzzy Systems 37 (4) (2019) 5417–5439. doi:10.3233/JIFS-190550.

[15] A. O. Almagrabi, S. Abdullah, M. Shams, Y. D. Al-Otaibi, S. Ashraf, A New Approach to q-Linear Diophantine Fuzzy Emergency Decision Support System for COVID-19, Journal of Ambient Intelligence and Humanized Computing 13 (3) (2022) 1687–1713. doi:10.1007/s12652-021-03130-y.

[16] S. Petchimuthu, M. J. Saravanakumar, K. Kumar, T. Senapati, Scaled q-rung orthopair fuzzy framework for optimizing municipal solid waste management: A case study of Pune, India, Applied Soft Computing (2026) 115916In press, journal pre-proof. doi:10.1016/j.asoc.2026.115916.

[17] J. Aczél, C. Alsina, Characterizations of Some Classes of Quasilinear Functions with Applications to Triangular Norms and to Synthesizing Judgements, Aequationes Mathematicae 25 (1) (1982) 313–315. doi:10.1007/BF02189626.

[18] T. Senapati, G. Chen, R. R. Yager, Aczel–Alsina Aggregation Operators and Their Application to Intuitionistic Fuzzy Multiple Attribute Decision Making, International Journal of Intelligent Systems 36 (12) (2021) 7802–7832. doi:10.1002/int.22684.

[19] T. Senapati, L. Martínez, G. Chen, Selection of Appropriate Global Partner for Companies Using q-Rung Orthopair Fuzzy Aczel–Alsina Average Aggregation Operators, International Journal of Fuzzy Systems 25 (2023) 980–996. doi:10.1007/s40815-022-01417-6.

[20] A. Hussain, K. Ullah, M.-S. Yang, D. Pamucar, Aczel-Alsina Aggregation Operators on T-Spherical Fuzzy (TSF) Information With Application to TSF Multi-Attribute Decision Making, IEEE Transactions on Fuzzy Systems 30 (12) (2022) 5427–5441. doi:10.1109/ACCESS.2022.3156764.

[21] H. Garg, Sine trigonometric operational laws and its based Pythagorean fuzzy aggregation operators for group decision-making process, Artificial Intelligence Review 54 (6) (2021) 4421–4447. doi:10.1007/s10462-021-10002-6.

[22] M. Qiyas, S. Abdullah, S. Khan, M. Naeem, Multi-attribute group decision making based on sine trigonometric spherical fuzzy aggregation operators, Granular Computing 7 (2022) 141–162. doi:10.1007/s41066-021-00256-4.

[23] H. Garg, K. Ullah, K. Ali, M. Akram, M. N. Abid, Multi-attribute decision-making based on sine trigonometric aggregation operators for T-spherical fuzzy information, Soft Computing 27 (22) (2023) 16793–16818. doi:10.1007/s00500-023-08899-y.

[24] A. Habib, Z. A. Khan, M. Riaz, D. Marinkovic, Performance Evaluation of Healthcare Supply Chain in Industry 4.0 with Linear Diophantine Fuzzy Sine-Trigonometric Aggregation Operations, Mathematics 11 (12) (2023) 2611. doi:10.3390/math11122611.

[25] M. Palanikumar, N. Kausar, D. Pamucar, V. Simic, Optimizing industrial robot selection using novel trigonometric Pythagorean fuzzy normal aggregation operators, Complex & Intelligent Systems 11 (2025) 453. doi:10.1007/s40747-025-02083-5.

[26] R. R. Yager, On Ordered Weighted Averaging Aggregation Operators in Multicriteria Decision-making, IEEE Transactions on Systems, Man, and Cybernetics 18 (1) (1988) 183–190. doi:10.1109/21.87068.

[27] F. Chiclana, F. Herrera, E. Herrera-Viedma, The Ordered Weighted Geometric Operator: Properties and Application in MCDM Problems, in: Technologies for Constructing Intelligent Systems 2, Vol. 90 of Studies in Fuzziness and Soft Computing, Physica, 2002, pp. 173–183. doi:10.1007/978-3-7908-1796-6_14.

[28] S. Saha, R. Chaki, IoT based smart waste management system in aspect of COVID-19, Journal of Open Innovation: Technology, Market, and Complexity 9 (2) (2023) 100048. doi:10.1016/j.joitmc.2023.100048.

[29] A. Ahuja, New Age Dustbins Deployed By New Delhi Municipal Council To Modernise Waste Collection, accessed on 15 July 2026 (2019).
URL https://swachhindia.ndtv.com/new-age-dustbins-deployed-by-new-delhi-municipal-council-to-modernise-waste-collection-35682/

[30] A. R. Chowdhury, Processing capacity gap galore, Delhi stinks: Shortfall of 6,000 tonnes/day, accessed on 17 July 2026 (July 2026).
URL https://www.newindianexpress.com/states/delhi/2026/Jul/02/processing-capacity-gap-galore-delhi-stinks

[31] Q. Cong, J. Lu, J. Tang, Enhancing Sustainable Waste-to-Energy: A Multi-Controlled Variable Prediction Model for Municipal Solid Waste Incineration, Sustainability 18 (5) (2026) 2616. doi:10.3390/su18052616.

[32] New Delhi Municipal Council, Smart City Proposal: DL-01-NDM, accessed on 08 July 2026 (2015).
URL https://www.ndmc.gov.in/smart_city_proposal.aspx

[33] S. S. Kapoor, A Paradigm Shift for Integrated Solid Waste Management: A Case Study of Delhi, in: Proceedings of the RACEE 2015 Conference, Vol. 4, IJERT, 2018, pp. 1–6, special Issue.
URL https://www.ijert.org/a-paradigm-shift-for-integrated-solid-waste-management-a-case-study-of-delhi

[34] P. Gawali, S. Shinde, J. Tambolkar, G. Shinde, S. Sawant, Smart IOT Based Dustbin and Waste Monitoring System, in: 2023 International Conference on Advances in Computation, Communication and Information Technology (ICAICCIT), IEEE, Faridabad, India, 2023, pp. 1–6. doi:10.1109/ICAICCIT60255.2023.10466052.

[35] M. N. Hossain, M. Rahman, IoT based garbage monitoring and management system, Review of Information Engineering and Applications 12 (1) (2025) 15–23. doi:10.18488/79.v12i1.4233.

[36] Municipal Corporation of Delhi, Expression of Interest (EOI) for Empanelment of Agency for Collection, Transportation and Processing of Waste: No. EE(EMS)/WZ/2026-27/D-184, accessed on 14 July 2026 (2026).
URL https://mcdonline.nic.in/portal/downloadFile/eoi_for_bwg_optimized_260619051241641.pdf

[37] A. Kumari, 333 CCTVs, Sensors: How Delhi Civic Body Keeps Watch On 17 Public Services, accessed on 14 July 2026 (2026).
URL https://www.ndtv.com/india-news/333-cctvs-sensors-how-delhi-civic-body-keeps-watch-on-17-public-services-11003066

[38] A. Rajput, Delhi Govt approves Rs. 100 crore for advanced traffic system to boost road safety, accessed on 15 July 2026 (2026).
URL https://infra.economictimes.indiatimes.com/news/urban-infrastructure/delhi-govt-invests-100-crore-in-advanced-traffic-system-for-enhanced-road-safety/128093528

[39] K. Hariharan, K. Jaya Suriya, S. Kishore Babu, B. P. Akilan, R. Vidhya, An AI-Enabled IoT-Based Waste Segregation Monitoring and Route Optimization System Using Google Maps for Urban Local Bodies, International Journal of Engineering Research & Technology (IJERT) 15 (4) (2026) 1–10, paper ID: IJERTV15IS041369. doi:10.5281/zenodo.19642221.

[40] The Statesman, EDMC inaugurates Material Recovery Facility in Shahdara South Zone, accessed on 17 July 2026 (2021).
URL https://www.thestatesman.com/cities/edmc-inaugurates-material-recovery-facility-shahdara-south-zone-1502977679.html

[41] C. Araujo-Andrade, et al., Review on the photonic techniques suitable for automatic monitoring of the composition of multi-materials wastes in view of their posterior recycling, Waste Management & Research 39 (5) (2021) 631–651. doi:10.1177/0734242X21997908.

[42] A. Daeyi, Support interventions for informal circular economy: A case study from delhi, india, European Journal of Spatial Development 23 (2) (2026) 38–76. doi:10.5281/zenodo.18467444.

[43] P. Singh, Centre clears expansion of Tehkhand waste-to-energy plant amid pollution concerns, accessed on 17 July 2026 (2026).
URL https://www.hindustantimes.com/cities/delhi-news/centre-clears-expansion-of-tehkhand-waste-to-energy-plant-amid-pollution-concerns-101781114667474.html

[44] R. Devraj, S. S. Sambyal, How Delhi's waste-to-energy plants are way off the mark, accessed on 17 July 2026 (2026).
URL https://www.downtoearth.org.in/waste/how-delhi-s-waste-to-energy-plants-are-way-off-the-mark-63026

[45] A. S. Meke, I. Dincer, A. Khalvati, Design and thermodynamic assessment of a sustainable waste to energy system for multiple useful outputs, Energy 351 (2026) 140773. doi:10.1016/j.energy.2026.140773.

[46] R. R. Yager, On a general class of fuzzy connectives, Fuzzy Sets and Systems 4 (3) (1980) 235–242. doi:10.1016/0165-0114(80)90013-5.

[47] J. Dombi, A general class of fuzzy operators, the demorgan class of fuzzy operators and fuzziness measures induced by fuzzy operators, Fuzzy sets and systems 8 (2) (1982) 149–163. doi:10.1016/0165-0114(82)90005-7.

[48] M. Frank, On the simultaneous associativity of F(x, y) and x+y-F(x, y), Aequationes Mathematicae 19 (1) (1979) 194–226. doi:10.1007/BF02189866.

Appendix A. Expert Linguistic Decision Matrices

The linguistic decision matrices from the four domain experts constitute the initial input to the proposed RT-SFAAST-based MAGDM framework, with each expert's evaluations of the five SWM alternatives under the seven decision criteria presented in Tables A.16–A.19.

Table A.16: Linguistic Decision Matrix provided by E_1.

	C_1 (Eff.)	C_2 (Cost)	C_3 (Effic.)	C_4 (Sustain.)	C_5 (Scalab.)	C_6 (Accept.)	C_7 (Maint.)
A_1	(VG, HR)	(P, LR)	(G, MR)	(VG, HR)	(F, MR)	(VG, MR)	(P, LR)
A_2	(VG, MR)	(P, HR)	(VG, MR)	(VG, HR)	(VG, LR)	(VG, MR)	(P, LR)
A_3	(VG, HR)	(G, HR)	(EX, MR)	(VG, HR)	(VG, MR)	(VG, LR)	(F, LR)
A_4	(VG, HR)	(VP, VHR)	(G, MR)	(VG, MR)	(F, LR)	(G, LR)	(VP, VLR)
A_5	(EX, VHR)	(EP, VHR)	(P, LR)	(VG, MR)	(G, MR)	(P, VLR)	(VP, VLR)

Table A.17: Linguistic Decision Matrix provided by E_2.

	C_1 (Eff.)	C_2 (Cost)	C_3 (Effic.)	C_4 (Sustain.)	C_5 (Scalab.)	C_6 (Accept.)	C_7 (Maint.)
A_1	(G, HR)	(VP, LR)	(F, MR)	(G, HR)	(F, MR)	(VG, MR)	(P, LR)
A_2	(VG, MR)	(VP, VHR)	(VG, MR)	(VG, HR)	(VG, LR)	(VG, MR)	(P, LR)
A_3	(VG, MR)	(F, HR)	(VG, MR)	(VG, MR)	(VG, HR)	(G, MR)	(F, MR)
A_4	(G, MR)	(EP, VHR)	(G, MR)	(VG, MR)	(F, LR)	(F, LR)	(P, VLR)
A_5	(VG, HR)	(EP, VHR)	(F, LR)	(VG, MR)	(G, MR)	(VP, VLR)	(EP, VLR)

Table A.18: Linguistic Decision Matrix provided by E_3.

	C_1 (Eff.)	C_2 (Cost)	C_3 (Effic.)	C_4 (Sustain.)	C_5 (Scalab.)	C_6 (Accept.)	C_7 (Maint.)
A_1	(VG, HR)	(P, MR)	(G, HR)	(VG, HR)	(G, MR)	(G, MR)	(P, LR)
A_2	(EX, MR)	(P, HR)	(VG, MR)	(EX, HR)	(EX, MR)	(VG, HR)	(P, LR)
A_3	(VG, HR)	(G, HR)	(EX, MR)	(VG, HR)	(EX, HR)	(VG, MR)	(F, LR)
A_4	(VG, HR)	(VP, VHR)	(VG, MR)	(VG, MR)	(G, LR)	(F, LR)	(VP, VLR)
A_5	(EX, HR)	(EP, VHR)	(P, LR)	(VG, MR)	(VG, MR)	(P, VLR)	(EP, VLR)

Table A.19: Linguistic Decision Matrix provided by E_4.

	C_1 (Eff.)	C_2 (Cost)	C_3 (Effic.)	C_4 (Sustain.)	C_5 (Scalab.)	C_6 (Accept.)	C_7 (Maint.)
A_1	(G, MR)	(P, MR)	(G, MR)	(VG, MR)	(F, MR)	(EX, MR)	(F, LR)
A_2	(VG, MR)	(P, HR)	(VG, MR)	(VG, MR)	(VG, MR)	(EX, MR)	(F, LR)
A_3	(VG, HR)	(G, MR)	(VG, MR)	(VG, HR)	(VG, MR)	(VG, MR)	(G, LR)
A_4	(G, HR)	(VP, VHR)	(F, MR)	(G, MR)	(F, LR)	(G, MR)	(VP, VLR)
A_5	(EX, HR)	(EP, VHR)	(F, VLR)	(VG, MR)	(G, MR)	(VP, VLR)	(EP, VLR)

Appendix B. Complete Collective RT-SFN Decision Matrix

Table B.20 presents the complete Collective Reliability T-Spherical Fuzzy Decision Matrix obtained using the proposed RT-SFAASTWA operator. For readability, the seven criteria are presented in four stacked blocks.

Table B.20: Complete Collective Reliability T-Spherical Fuzzy Decision Matrix.

	C_1	C_2
A_1	$((0.813, 0.137, 0.190), (0.826, 0.174, 0.174))$	$((0.711, 0.421, 0.350), (0.389, 0.360, 0.611))$
A_2	$((0.894, 0.083, 0.109), (0.700, 0.300, 0.300))$	$((0.711, 0.421, 0.350), (0.131, 0.000, 0.869))$
A_3	$((0.850, 0.100, 0.150), (0.826, 0.174, 0.174))$	$((0.360, 0.219, 0.703), (0.203, 0.174, 0.797))$
A_4	$((0.813, 0.137, 0.190), (0.826, 0.174, 0.174))$	$((0.839, 0.521, 0.190), (0.000, 0.000, 1.000))$
A_5	$((0.938, 0.059, 0.063), (1.000, 0.000, 0.000))$	$((0.900, 0.600, 0.100), (0.000, 0.000, 1.000))$

	C_3	C_4
A_1	$((0.727, 0.219, 0.283), (0.756, 0.244, 0.244))$	$((0.833, 0.117, 0.168), (0.826, 0.174, 0.174))$
A_2	$((0.850, 0.100, 0.150), (0.700, 0.300, 0.300))$	$((0.894, 0.083, 0.109), (0.826, 0.174, 0.174))$
A_3	$((0.920, 0.069, 0.082), (0.700, 0.300, 0.300))$	$((0.850, 0.100, 0.150), (0.826, 0.174, 0.174))$
A_4	$((0.771, 0.179, 0.243), (0.700, 0.300, 0.300))$	$((0.833, 0.117, 0.168), (0.700, 0.300, 0.300))$
A_5	$((0.543, 0.344, 0.530), (0.522, 0.478, 0.478))$	$((0.850, 0.100, 0.150), (0.700, 0.300, 0.300))$

	C_5	C_6
A_1	$((0.660, 0.268, 0.378), (0.700, 0.300, 0.300))$	$((0.885, 0.095, 0.120), (0.700, 0.300, 0.300))$
A_2	$((0.894, 0.083, 0.109), (0.640, 0.360, 0.360))$	$((0.894, 0.083, 0.109), (0.756, 0.244, 0.244))$
A_3	$((0.894, 0.083, 0.109), (0.796, 0.204, 0.204))$	$((0.833, 0.117, 0.168), (0.673, 0.327, 0.327))$
A_4	$((0.660, 0.268, 0.378), (0.550, 0.450, 0.450))$	$((0.699, 0.242, 0.324), (0.600, 0.400, 0.400))$
A_5	$((0.786, 0.164, 0.217), (0.700, 0.300, 0.300))$	$((0.359, 0.444, 0.713), (0.400, 0.600, 0.600))$

	C_7
A_1	$((0.624, 0.370, 0.436), (0.450, 0.450, 0.550))$
A_2	$((0.624, 0.370, 0.436), (0.450, 0.450, 0.550))$
A_3	$((0.429, 0.268, 0.630), (0.422, 0.400, 0.578))$
A_4	$((0.778, 0.471, 0.277), (0.600, 0.600, 0.400))$
A_5	$((0.885, 0.571, 0.121), (0.600, 0.600, 0.400))$